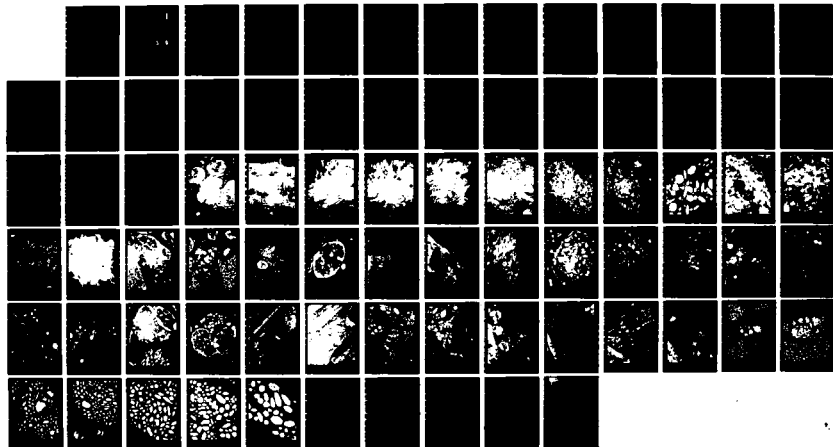BIOLOGICAL APPLICATIONS AND EFFECTS OF OPTICAL MASERS
(U) MEDICAL COLL OF VIRGINIA RICHMOND W T HAM ET AL.
SEP 78 DADA17-72-C-2177

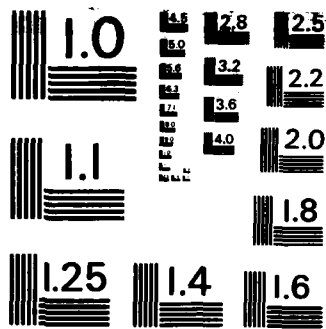MICROCOPY RESOLUTION TEST CHART
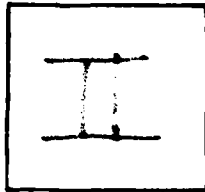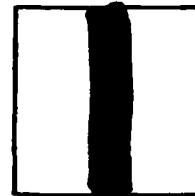
NATIONAL BUREAU OF STANDARDS-1963-A

LEVEL

INVENTORY

AD-A141 008

DTIC ACCESSION NUMBER

Annual Rpt.,
1 Sep.'77 - 31 Aug.'78
DOCUMENT IDENTIFICATION

Contract DADA17-22-C-2177   Sep.'78

DISTRIBUTION STATEMENT

ACCESSION FOR

NTIS	GRA&I	☒
DTIC	TAB	☐
UNANNOUNCED		☐
JUSTIFICATION		

BY
DISTRIBUTION /
AVAILABILITY CODES

DIST	AVAIL AND/OR SPECIAL
A/1	

DISTRIBUTION STAMP

DTIC
ELECTE
S MAY 14 1984
D

D
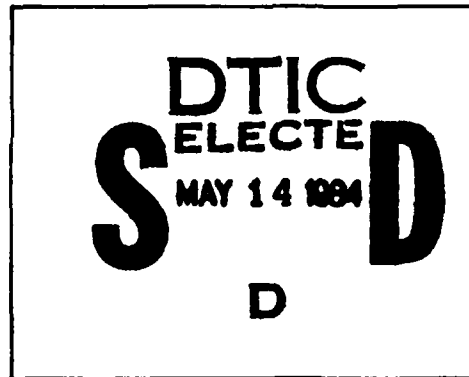
DATE ACCESSIONED

84   05   10   036

DOCUMENT PROCESSING SHEET

DTIC FORM 70A
OCT 79

AD _____

BIOLOGICAL APPLICATIONS AND EFFECTS OF OPTICAL MASERS

ANNUAL REPORT

William T. Ham, A. M. Clarke,
H. A. Mueller and J. J. Ruffolo

September 1978

Supported by

US ARMY MEDICAL RESEARCH AND DEVELOPMENT COMMAND
Fort Detrick, Frederick, Maryland   21701

Contract No. DADA17-72-C-2177

The Medical College of Virginia
1200 East Broad Street
Richmond, Virginia   23298

Approved for public release; distribution unlimited

AD-A141 008

REPORT DOCUMENTATION PAGE		READ INSTRUCTIONS BEFORE COMPLETING FORM
REPORT NUMBER	2. GOVT ACCESSION NO.	3. RECIPIENT'S CATALOG NUMBER
4. TITLE (and Subtitle) BIOLOGICAL APPLICATIONS AND EFFECTS OF OPTICAL MASERS		5. TYPE OF REPORT & PERIOD COVERED Annual – 1 September 1977 – 31 August 1978
		6. PERFORMING ORG. REPORT NUMBER
7. AUTHOR(s) William T. Ham, Jr., Ph.D.		8. CONTRACT OR GRANT NUMBER(s) DADA17-72-C-2177
9. PERFORMING ORGANIZATION NAME AND ADDRESS Virginia Commonwealth University The Medical College of Virginia Richmond, Virginia 23298		10. PROGRAM ELEMENT, PROJECT, TASK AREA & WORK UNIT NUMBERS 62777A.3E162777A878.BA.206
11. CONTROLLING OFFICE NAME AND ADDRESS US Army Medical Research and Development Command Fort Detrick Frederick, Maryland 21701		12. REPORT DATE September 1978
		13. NUMBER OF PAGES 76
14. MONITORING AGENCY NAME & ADDRESS(if different from Controlling Office)		15. SECURITY CLASS. (of this report) Unclassified
		15a. DECLASSIFICATION/DOWNGRADING SCHEDULE

16. DISTRIBUTION STATEMENT (of this Report)

Approved for public release; distribution unlimited.

17. DISTRIBUTION STATEMENT (of the abstract entered in Block 20, if different from Report)

18. SUPPLEMENTARY NOTES

19. KEY WORDS (Continue on reverse side if necessary and identify by block number)

20. ABSTRACT (Continue on reverse side if necessary and identify by block number)

DD FORM 1 JAN 73 1473 EDITION OF 1 NOV 65 IS OBSOLETE

Abstract:

The histological investigations of the photochemical lesion produced
in the rhesus retina by blue light (441 nm) have been completed for post-
exposure times ranging from one hour to ninety days. The results have been
submitted to INVESTIGATIVE OPHTHALMOLOGY for publication (see Appendix A)
and were also reported at the annual ARVO meeting in May 1978 (see Appendix
B). Ultrastructural studies of the lesion by transmission EM are well ad-
vanced for periods of 2, 5, and 6 days postexposure. Visual acuity studies
continue, one additional animal having been trained during the last six
months. Spectral sensitivity tests at 20 nm intervals have been completed
for the spectral range 420-620 nm on two animals. The latency of response
to the light stimulus has been studied on three animals. The original study
on visual acuity after exposure to blue light has been accepted for publi-
cation in VISION RESEARCH (see Appendix C). To further elucidate the dif-
ferential effects on the retina of short vs long wavelength CW radiation
the simulated solar spectrum 300-1400 nm was divided into two spectral bands,
400-800 nm and 700-1400 nm. The radiant exposures required to produce very
mild lesions in 1, 10, 100 and 1000 s were determined on eight rhesus monkeys
for each spectrum, i.e. 300-1400 nm, 400-800 nm, 700-1400 nm. This study,
as well as a summary of the photopathology of the photochemical lesion and
its effects on visual acuity, were presented at a symposium on "Light Damage
to the Retina and Retinal Pigment Epithelium" at the 6th Annual Meeting of
the American Society for Photobiology, University of Vermont, 13 June 1978.
The manuscript has been submitted for publication in PHOTOCHEMISTRY and
PHOTOBIOLOGY (see Appendix D). An additional study is being conducted to
determine the radiant exposures required to produce a mild retinal lesion
in the waveband 400-735 nm by using nine sharp cut filters at 400-735,
435-735, 455-735, 485-735, 515-735, 545-735, 575-735, 625-735 and 675-735
nm. Minimal lesions produced by these nine wavebands have been determined
in three out of ten animals. Data to date indicate radiant exposures
ranging from 200 J/cm^2 for the 400-735 nm band to 1350 J/cm^2 for the 675-
735 nm band. A preliminary study has begun on the effects of the Ga-As
injection laser on the rhesus retina. Results to date indicate a very
mild funduscopically visible lesion approximately 150 μm in diameter 24
hours after exposure to a combined white light (Fundus camera, position 3)
and Ga-As laser at a prf of 1200 Hz. The calculated radiant exposure of
the retina to the laser was 65 J/cm^2 for a 500 s exposure. No lesion was
funduscopically visible after a 500 s exposure to the Ga-As laser alone.
Attempts are underway to develop a mathematical formula which will give
the radiant exposure for a minimal lesion as a function of wavelength,
exposure time and power level. Results to date are encouraging. As yet,

no exposures of animals to the UV wavebands 330-420 nm and 330-490 nm have been made, but the necessary apparatus (animal chair, optical system and photodetector) has been assembled and exposures will begin during the autumn. The low level photodetector for reflectance and fluorescence measurements in the lens and illumination measurements in visual acuity testing has been completed. The linearity of the instrument was checked at the USAEHA at Edgewood and calibration procedures are now in progress. Little progress was made during the year on extending the action spectrum for retinal lesions into the near UV. The cataract operation on the rhesus eye has proven successful and aphakic eyes are now available, but numerous equipment failures rendered the argon laser non-functional during most of the year, thus preventing progress on both the action spectrum and the study of pulsed vs CW radiation effects on the retina. Accordingly the main thrust of our research has been on visible vs infrared effects using the xenon lamp optical system while our laser systems were being repaired.

TABLE OF CONTENTS

TABLE 1

Paramacular response to short wavelength light (441 nm) after irradiation for 1,000 seconds (16.7 minutes)

age of lesion	radiant exposure (J/cm²)	description of response
< 1 hour	33	Neural retina, pigment epithelium, choroid appear normal
< 1 hour	46	Neural retina: several nuclei with varying degrees of chromatin clumping in ONL, a few dense cones, a cone nucleus below OLM; pigment epithelium and chorid appear normal.
1 day	33	Neural retina: a few rod nuclei with chromatin clumping, a few dense cones and rods; pigment epithelium and choroid appear normal.
1 day	35	Neural retina, pigment epithelium, choroid appear essentially normal.

1. Photopathology of Retinal Lesions Induced by Short Wavelength Light

To date we have thoroughly analyzed the histological response of 20 para-macular lesions (more than 3000 thick sections for light microscopy and 322 light micrographs) at postexposure times ranging from <1 hour to 90 days. These data are summarized in Tables 1-5 and Figure 1. These tables and the general scheme diagram are updated to give several new observations, particularly about the neural retina. A brief report of these results has been submitted to INVESTIGATIVE OPHTHALMOLOGY for publication (see Appendix A). Also, these results were reported at the annual ARVO meeting at Sarasota, Florida in May 1978 (see Appendix B).

The ultrastructural study of 7 paramacular lesions is progressing well (35 grids of thin sections; 189 electron micrographs covering a 2 day, 5 day, and 6 day lesion). Three of the lesions have been studied to date. These are designated by EM in Tables 2 and 3. The four remaining lesions for ultra-structural analysis are designated by (EM) in Tables 3-5.

A sampling of the ultrastructural analysis to date is given in Figures 2-45. Figure Legends are included for each micrograph. Figures 2-16 illustrate portions of a 2 day lesion (441 nm at 33 J/cm^2 for 1000 s) giving observations on the neural retina (macrophage in the outer nuclear layer, and dense cones), pigment epithelium (melanosomes in various stages of degeneration; bundles of tubular membranes in the cytoplasm; vesiculation of the cytoplasm), and choroid (eosinophils and other leucocytes; macrophages; apparent damage and degeneration of melanosomes in melanocytes).

Figures 17-30 show portions of a 5 day lesion (435 nm at 35 J/cm^2 for 1000 s) giving data about the neural retina (macrophage in the outer plexiform layer next to the outer nuclear layer; dense cone cytoplasm; membrane tubules, discs, and vesicles in a cone ellipsoid), pigment epithelium (macrophages in the subretinal space contain degenerating melanosomes, membrane debris, and lipid-like bodies; RPE cells are very hypopigmented; some cells have a large amount of smooth endoplasmic reticulum and a dense flocculent material; cell junctions are observed despite some cell stacking and interdigitation; a cell with a strange grouping of 3 fuzzy ribbon or rod-like objects; some melanosomes show numerous alveolar spaces of low density referred to as "blanched spots"), and choroid (eosinophils and other leucocytes; macrophages; blanched spots in melanosomes of melanocytes).

Figures 31-45 illustrate parts of a 6 day lesion (441 nm at 33 J/cm^2 for 1000 s) making observations on the neural retina (membrane configurations in a cone outer segment that could manifest either degeneration of the OS or a stage of regeneration), pigment epithelium (macrophages in the subretinal space contain degenerating melanosomes, some of which have blanched spots, membrane debris, and lipid-like bodies; some RPE cells have well-developed Golgi complexes; some cells are very hypopigmented, others have degenerating melanosomes; some cells have well-developed smooth endoplasmic reticulum; cell junctions are seen despite cell stacking and interdigitation), and choroid (macrophages; melanosomes of the melanocytes have many blanched spots; many melanosomes show stages of degeneration).

At this stage of the ultrastructural analysis the observations and interpretations must be taken as preliminary. When study of the 4 remaining paramacular lesions (Tables 3-5) is completed a more integrated analysis of the ultrastructural observations can be made. Such an analysis added to the light microscopic histological data should allow a rather detailed characterization of the retinal response to blue light.

TABLE 2

Paramacular response to short wavelength light (441 nm) after irradiation for 1,000 seconds (16.7 minutes) or 10,000 seconds (2.8 hours)

age of lesion	radiant exposure (J/cm^2)	duration	description of response
2 days EM	33	1,000 s	(pigmentary retinochoroiditis) <u>Neural retina</u>: a few rod nuclei have clumped chromatin, debris-laden macrophages observed at level of inner segments, a few seen above OLM, some dense cones, a few cone ellipsoids conspicuously damaged, little or no OS damage; <u>Pigment epithelium</u>: extensive disruption, macrophages in PE and subretinal space engorged with melanin and membrane debris;. <u>Choroid</u>: inflammation, minimal edema, choriocapillaris partially occluded by leucocytes, venous system in area of lesion shows accumulation of leucocytes, macrophages contain ingested melanin.
2 days	35	1,000 s	(pigment epithelitis) <u>Neural retina</u>: no chromatin clumping, a few cone ellipsoids conspicuously damaged, no obvious OS damage; <u>Pigment epithelium</u>: some disruption, macrophages in PE and sub-retinal space contain melanin and membrane debris; <u>Choroid</u>: little or no inflammation, mild edema.
2 days	50	10,000 s	(pigmentary retinochoroiditis) <u>Neural retina</u>: very few rod nuclei with chromatin clumping, a few dense cones, very few damaged cone ellipsoids, no obvious OS damage, debris-laden macrophages at level of inner segments, some seen above OLM; <u>Pigment epithelium</u>: some disruption, macrophages in PE and subretinal space contain melanin and membrane debris; <u>Choroid</u>: some inflammation, mild edema, choriocapillaris has few leucocytes, macrophages contain melanin.
3 days	35	1,000 s	(pigmentary retinochoroiditis) <u>Neural retina</u>: no chromatin clumping in ONL nor conspicuous ellipsoid damage, several dense cones, little or no OS damage; <u>Pigment epithelium</u>: some disruption, debris-laden macrophages in PE and subretinal space; <u>Choroid</u>: mild inflammation, moderate edema, choriocapillaris has few leucocytes.

TABLE 4

Paramacular response to short wavelength light (441 nm and 435 nm) after irradiation for 1,000 seconds (16.7 minutes)

age of lesion	wavelength (nm)	radiant exposure (J/cm^2)	description of response
10 days (EM)	441	35	(pigment epithelitis) Neural retina: very few rod nuclei with chromatin clumping, some damaged cone ellipsoids, very few dense cones, some indication of fewer cones, localized disorientation of some OS, macrophages in OPL and IPL; Pigment epithelium: somewhat disrupted, debris-laden macrophages in PE and subretinal space; Choroid: no inflammation, little or no edema.
11 days	441	35	Neural retina: very few rod nuclei with clumped chromatin, some moderately dense cones, no damaged ellipsoids, some indication of fewer cones, OS appear shorter in area of lesion, chromatin clumping in nuclei at level of horizontal cells, macrophages in OPL, INL (level of horizontal cells), and IPL; Pigment epithelium: mostly regenerated and restored to single layer of cells, large macrophages in subretinal space; Choroid: no inflammation, little or no edema.
11 days (EM)	435	35	Neural retina: upward buckling near border of lesion, some rod nuclei with chromatin clumping, several dense cones and rods, macrophages limited to OPL, OS shorter in lesion, some very short and disoriented, several Muller cells very dense, chromatin clumping at level of horizontal cells; Pigment epithelium: mostly regenerated, some areas extremely hypopigmented, debris-laden macrophages in subretinal space; Choroid: no inflammation, little or no edema.

TABLE 3

Paramacular response to short wavelength light (441 nm and 435 nm) after irradiation for 1,000 seconds (16.7 minutes)

age of lesion	wavelength (nm)	radiant exposure (J/cm^2)	description of response
5 days	441	35	(pigment epitheliitis) Neural retina: no chromatin clumping in ONL, some dense cones, a few damaged cone ellipsoids, little or no OS damage, no macrophages at level of inner segments; Pigment epithelium: some disruption, debris-laden macrophages in PE and subretinal space; Choroid: no inflammation, little or no edema, choriocapillaris has few leucocytes.
5 days EM	435	33	(pigment epitheliitis) Neural retina: upward buckling near borders of lesion, very few rod nuclei with chromatin clumping, little conspicuous cone cell damage, OS appear damaged and disoriented, no macrophages at level of inner segments; Pigment epithelium: considerable disruption of PE, a few mitotic figures, debris-laden macrophages in PE and subretinal space; Choroid: very mild inflammation, little or no edema, choriocapillaris has few leucocytes.
6 days EM	441	33	(pigmentary retinochoroiditis) Neural retina: a few rod nuclei with chromatin clumping, little evidence of cone cell damage, OS appear damaged and disoriented, macrophages in and near ONL; Pigment epithelium: considerable disruption, no mitotic figures observed, debris-laden macrophages in PE and subretinal space; Choroid: considerable choroidal inflammation in central portion of image area, little or no edema, choriocapillaris has numerous leucocytes, mitotic figures and debris-laden macrophages.
6 days (EM)	441	35	(pigment epitheliitis) Neural retina: a few rod nuclei with clumped chromatin, some damaged cone ellipsoids, some dense cones, considerable OS disorientation, macrophages in INL, OPL, ONL, upward buckling near border of lesion; Pigment epithelium: considerable disruption, mild hyperplasia, numerous mitotic figures, debris-laden macrophages in PE and subretinal space; Choroid: very mild inflammation, little or no edema, choriocapillaris has few leucocytes.

-8-

TABLE 5

Paramacular response to short wavelength light (441 nm and 435 nm) after irradiation for 1,000 seconds (16.7 minutes)

age of lesion	wavelength (nm)	radiant exposure (J/cm^2)	description of response
30 days	441	33	Neural retina: no overt signs of damage; Pigment epithelium: well regenerated, hypopigmented, large macrophages in subretinal space; Choroid: no inflammation, no edema.
30 days (EM)	441	35	Neural retina: very few rod nuclei with chromatin clumping, several moderately dense cones, a few dense rods, very few damaged cone ellipsoids, some damaged rod ellipsoids, some indication of fewer cones, OS appear normal; Pigment epithelium: well regenerated, hypopigmented, large macrophages in subretinal space, a few in PE agains Bruch's membrane; Choroid: no inflammation, little or no edema.
30 days	435	35	Neural retina: very few rod nuclei with clumped chromatin, several dense cones, some beyond border of lesion, some indication of fewer cones, OS appear normal; Pigment epithelium: well regenerated, hypopigmented, large macrophages in subretinal space, a few in PE against Bruch's membrane; Choroid: no inflammation, no edema.
60 days	441	33	Neural retina: no overt signs of damage, OS appear somewhat shorter in area of lesion; Pigment epithelium: well regenerated, hypopigmented, a few small macrophages in subretinal space, remaining debris-laden macrophages in PE, some against Bruch's membrane; Choroid: no inflammation, no edema.
90 days	441	33	Neural retina: no signs of damage; Pigment epithelium: appears fully regenerated, hypopigmentation is subtle, no large macrophages in subretinal space, very few remaining debris-laden macrophages in PE against Bruch's membrane; Choroid: no inflammation, no edema.

FIGURE 1   A General Scheme of Retinal Photopathology.

-11-

2. Relationship Between Retinal Lesions Produced by Short Wavelength Light and Visual Performance in the Trained Rhesus Monkey

Visual performance as a function of blue light exposure levels, discussed in the 1976-77 report has been expanded and accepted for publication in *Vision Research*. The manuscript appears as Appendix C of this report. Since that report, we have developed two additional tests of visual performance which should increase the accuracy of our results. These are a latency of response test and a spectral sensitivity test. Preliminary data on these new tests are discussed below.

A. Response Latency:

The interval between the presentation of the Landolt ring visual task target, and the response of the monkey by striking the lever will be hereafter referred to as the "response latency" or response time. This interval is that time that the monkey takes to recognize that the ring target has appeared, decide the orientation of the gap in the ring, and strike the lever. In the treatment of the data, no distinction is made as to whether the response is correct or incorrect. Data for the two exposed animals are given in Tables 6 and 7. The mean, $\bar{x}$ (in seconds), standard deviation, S_x

$$S_x = ((\Sigma_i x_i^2 - n_i \bar{x}^2)(n-1)^{-1})^{\frac{1}{2}}$$

and standard error of the mean, $S_{\bar{x}}$

$$S_{\bar{x}} = S/n^{\frac{1}{2}}$$

are presented.

Comparing the average of the data for 4 days in early Fall of 1977 and individual data for two days in late Spring of 1978 for the animal exposed to 60 and 90 J/cm^2 (Table 6) in the fovea shows no significant difference in the percentage of correct responses to the presentation, or the response times for the similar sizes. Further, for the two days where the data is for "random" presentations (meaning the gap size and orientation were randomly presented) and ordered (gap sizes presented in sets of eight similar gap sizes, with orientation random) there is no significant difference in the response times. Although an apparent difference in the percentage correct exists between the random and ordered presentations, this difference is within the standard deviation for data over a four month period, and well within the extremes over this period.

Examination of the data (Table 7) for the animal exposed to 30 and 60 J/cm^2 in the fovea indicates that there is no significant difference between the acuity (based on percentage correct responses) of the two eyes, nor on the response times in early Fall 1977 to late Spring 1978, nor in the ordered versus random presentation of the targets.

Table 6

The Mean Response Times in Seconds for the Right and Left Eyes of Monkey 1
For Random and Ordered Presentations

	Right Eye			Left Eye		
Target Size (min. of arc)	0.5	1.0	1.5	1.0	1.5	2.0
Random Presentation (ave. of 4 sessions – Fall 77)						
$\bar{x}$	3.52	0.84	0.72	2.31	1.29	1.02
s_x	0.77	0.21	0.16	0.81	0.39	0.25
$s_{\bar{x}}$	0.14	0.04	0.03	0.14	0.07	0.02
% correct	57	98.5	97.9	72	91.5	92.5
Random Presentation (1 session – Spring 78)						
$\bar{x}$	2.84	0.89	0.72	1.32	1.16	0.91
s_x	0.92	0.23	0.12	0.37	0.27	0.17
$s_{\bar{x}}$	0.16	0.04	0.02	0.07	0.06	0.04
% correct	56	91	100	66	83	92
Ordered Presentation (1 session – Spring 78)						
$\bar{x}$	2.34	0.88	0.77	1.26	0.94	0.83
s_x	1.40	0.21	0.12	0.50	0.21	0.20
$s_{\bar{x}}$	0.35	0.04	0.02	0.09	0.04	0.04
% correct	50	97	100	78	97	100

Table 7

The Mean Response Times in Seconds for the Right and Left Eyes of Monkey 2
For Random and Ordered Presentations

	Right Eye			Left Eye		
Target Size (min. of arc)	0.5	1.0	1.5	0.5	1.0	1.5
Random Presentation (ave. of 4 sessions – Fall 77)						
$\bar{x}$	1.51	0.67	0.61	1.55	0.66	0.61
s_x	0.47	0.09	0.08	0.45	0.08	0.08
$s_{\bar{x}}$	0.09	0.02	0.01	0.08	0.01	0.01
% correct	69	98.5	98.5	72	99	98.5
Random Presentation (1 session – Spring 78)						
$\bar{x}$	1.11	0.72	0.62	1.46	0.86	0.66
s_x	0.39	0.16	0.12	0.49	0.59	0.16
$s_{\bar{x}}$	0.07	0.03	0.02	0.09	0.05	0.03
% correct	78	94	100	63	94	100
Ordered Presentation (1 session – Spring 78)						
$\bar{x}$	1.10	0.78	0.70	1.11	0.85	0.67
s_x	0.48	0.20	0.14	0.47	0.22	0.10
$s_{\bar{x}}$	0.08	0.04	0.03	0.08	0.04	0.02
% correct	72	100	97	69	94	100

To ensure that there are no "learning" or fatigue" factors during the experiments, a number of runs were made in which one eye of each of the subjects was run twice as opposed to running first one eye and then the other. No significant difference appeared between the first and second run for either for percentage correct (no "learning"), nor the response times (no "fatigue"). Even with this assurance, the first eye run was alternated each session.

Additionally, the animals were occasionally shown blank frames in which no target appeared, to ascertain if the animal would have a favorite lever, or if the animal would respond by striking random levers. In all cases the animal merely struck the lever nearest his restrained hand. The time of response for the no-target presentation varied markedly between the two monkeys. The one with reduced vision in one eye responded to the blank frame in a time comparable to that for the 0.5 (20/10) target for the eye with "normal" vision. However, the animal with normal vision in both eyes responded to the no-target frame in a time shorter than the mean for the 0.5' target, but longer than that for the 1.0' target.

Conclusions:

1. Response time in the visual acuity task, as used in the series of experiments described here, is a significant parameter for the determination of visual acuity in animals trained for this specific task. The day by day variability of this response time as a function of acuity can be shown to be similar to that in the percentage responses correct.

2. The response time for ordered size presentations is not significantly different from that for random size presentations, making the response latency parameter a useful one when diminishing stepwise the light level in spectral acuity tests.

3. There is a significant correlation between the response times for the similar target sizes for the two larger (20/20 and 20/30) targets in the eyes of the animals which have not been radiantly exposed to the point of the production of a visual decrement. However, the animal which has been exposed in one eye to a light level sufficient to cause a visual decrement shows a longer response latency to the 20/10 target in his unimpaired eye, indicating that the visual decrement in the impaired eye may have taught him a certain tenacity in searching for the target. This supposition is further supported by a third animal which has not been mentioned in this section, which has been in the training program less than 9 months, has not yet been exposed to blue light (441 nm), and which exhibits a much smaller response latency difference between the large and small targets than either of the two animals which have been exposed.

B. Spectral Acuity:

The two trained animals whose visual decrement due to blue light exposure is discussed in Appendix C are being run in a similar protocol in which the acuity of the animal is tested as a function of target color and the chamber/surround illumination level. At this point we have obtained the target color vs. target illuminance for a total darkness surround. Anomalies seem to exist in the red end of the spectrum, although we cannot be certain because, to date, we have not been able to get an absolute measure of the intensity of the target illuminance as a function of wavelength. The low light level meter, discussed in Section 3 will be used to obtain these data. The CIE curve and data from a third animal which has been in our training program for the last 8 months will be used to ascertain what spectral anomalies have developed from the blue light exposure.

3. Low Light Level Meter

We have completed the construction and initial calibration of a low level light meter, suitable for the measurement of both the illumination level of the visual acuity targets and the relative reflectance from the lens/cornea.

In conjunction with Mr. Sliney at the USAEHA, we have demonstrated that this device is linear over at least 4 orders of magnitude. This instrument will be calibrated using an NBS standard of irradiance and a series of Melles-Griot 10 nm filters (410 nm to 680 nm).

Essentially, this instrument integrates the signal from a Silicon detector over a digitally adjustable timing interval. The integrated signal is read out on a $3\frac{1}{2}$ digit panel meter to a greater accuracy than the calibration of the NBS standard.

This scheme shows excellent promise, and has not been used commercially elsewhere. As soon as the instrument has been completely calibrated and we ascertain that all "bugs" have been worked out, a detailed technical description will be submitted to the Project officer and a suitable scientific instrumentation journal.

CORNEAL POWER (WATTS)

Waveband (nm) Monkey	400-735	435-735	455-735	485-735	515-735	545-735	575-735	625-735	675-735
76-22	.004	.0355	.007	.0091	.013	.017	.0228	.0244	.025
76-16	.004	.045	.0089	.010	.0123	.013	.0216	.030	.031
76-25	.00645	.0061	.0072	.0113	.0128	.0185	.0227	.0236	.0275
AVG	.0052	.0046	.0077	.0101	.0127	.0162	.0224	.0260	.0278
	$\pm$.0012	$\pm$.0014	$\pm$.001	$\pm$.0011	$\pm$.0004	$\pm$.0028	$\pm$.0007	$\pm$.0035	$\pm$.003
	23.1%	30.4%	13.0%	10.9%	3.2%	17.3%	3.1%	13.5%	10.8%

RETINAL IRRADIANCE (Wcm^{-2})

	400-735	435-735	455-735	485-735	515-735	545-735	575-735	625-735	675-735
	2.11	2.03	3.29	4.64	5.98	7.55	10.6	12.4	13.5

RETINAL EXPOSURE (Jcm^{-2})

	400-735	435-735	455-735	485-735	515-735	545-735	575-735	625-735	675-735
	211	203	329	464	598	755	1,064	1,235	1,348

Table 8

All exposures 100 s, 500 um image diameter.

Incomplete data on 9 spectral bands(400 -735nm) , corneal power, retinal irradiance and retinal exposure. Data follows retinal sensitivity data of Ham,et al(1976)

4. Retinal Damage as a Function of Wavelength

This study as first reported in Nature 1976 has been continued and expanded by using the Xenon lamp optical system with quartz optics. Our progress up to the present was reported at a symposium on "Light Damage to the Retina and Retinal Pigment Epithelium" during the annual meeting of the American Photo-biology Society at Burlington, Vt., June 13, 1978. Our invited paper entitled "Sensitivity of the Retina to Radiation Damage as a Function of Wavelength" (see Appendix D) will be published in PHOTOCHEMISTRY and PHOTOBIOLOGY. In this paper we review the action spectrum and photopathology of the photochemical lesion as investigated in the rhesus monkey, describing how it differs from a thermal lesion and how it affects visual performance. The effect of wavelength on the type of retinal lesion is discussed in some detail. Using image sizes on the rhesus retina which correspond to the image size of the sun on the human retina (159 mm diam.), we have produced minimal lesions at exposure times of 1, 10, 100 and 1000 s for three spectral bandwidths, 300-1400 mm, 400-800 mm and 700-1400 mm. The results demonstrate that CW near infrared radiation plays only a minor role in solar retinopathies and that solar retinitis and eclipse blindness are primarily photochemical events produced by the short wavelength visible component in the solar spectrum.

To further elucidate the effect of wavelength on the production of damage in the rhesus retina we have employed the Xenon optical system to begin a series of 100 s exposures for the spectral bank 400-735 mm using 9 sharp cut filters to obtain the following wavebands: 400-735, 435-735, 455-735, 485-735, 515-735, 545-735, 575-735, 625-735 and 675-735. The results to date on 3 monkeys are shown in Table 8. Radiant exposures required to produce a minimal lesion range from 203 J/cm^2 for the 435-735 nm waveband to 1348 J/cm^2 for the 675-735 nm waveband. The reason that the 400-735 nm band requires 211 J/cm^2 as compared to 203 J/cm^2 for the 435-735 nm spectrum is probably because wavelengths between 400 and 435 nm are almost completely absorbed by the cornea, aqueous and lens, especially by the latter. The type of lesion progresses from a predominately photochemical type for the short wavelength bands to a predominately thermal type for the red light band 675-735 nm. This is particularly noticeable in fundoscopy where the lesion size remains at 500 nm for the short wavelengths and begins to become smaller as we approach the longer wavelengths where thermal effects predominate.

-17-

5. Preliminary Experiments with Ga-As Injection Lasers.

Although research on the effects of Ga-As radiation on the retina were
not included in our original protocol we have diverted some of our research
time to this problem because of its urgency in the Army training programs
of the future. This problem was first presented to us last September 1977
when we visited the laser research group at LAIR. In an attempt to reproduce
some of their findings we have exposed a rhesus eye to a Ga-As laser having
the following physical parameters: 12000 púlses/s, 2.1 x 10^{-8} J/pulses,
905 nm. Exposure times were 60, 100 and 500 s. The spot size on the retina
as judged funduscopically by a lesion obtained at 24 hours postexposure was
approximately 150 nm in diameter and appeared to be round. This lesion was
produced with the fundus camera set on position 3 which produces a 30° cone
of white light on the retina. It is estimated that the 500 second exposure
resulted in a radiant exposure to the retina of 650 J/cm^2. Exposure to the
laser for 500 s without the fundus camera illumination did not produce a
lesion; exposures to the laser for 60 and 100 s did not produce a lesion with
or without the fundus camera. These preliminary results are difficult to
interpret and until we have investigated the phenomenon more thoroughly
further discussion is not warranted.

6. Mathematical Models to Describe the Thermal and Photochemical Components of the Retinal Lesion.

In an attempt to further our understanding of the mechanisms of photic
damage to the retina for long time exposures we have undertaken the construction
of a simple mathematical model, which we will expand on in future contract
periods.

The function E_o $(W \cdot cm^{-2})$ can be described as a function of wavelength by

$$E_o = (Ae^{-a\lambda} + Be^{-b\lambda})^{-1}$$

where E_o is the retinal power density as described by Ham, et al., (Nature 260:
153, 1976), the first term describes the photochemical damage and the second
the thermal damage. At long wavelengths the A term is negligible, indicating
minimal photochemical interaction. At short wavelengths, however, while the
B term becomes small, it is not negligible, indicating a thermal contribution
(perhaps enhancement) in the production of the lesion.

The fit obtained to our data is considerably better than order of magnitude
after the first iterative step. This approach, while elementary in concept,
seems more in keeping with the biophysical realities of exposures greater
than 1 second that the time-temperature models for short exposures, or the
thermal models previously used for predicting retinal lesions. Unfortunately,
we have not yet been able to fit the coefficients to meaningful formulae as
functions of exposure time.

7. Papers Delivered

A. Sarasota, Fla., ARVO, May 1978, J.J. Ruffolo, "Photopathology of retinal lesions in rhesus monkeys induced by extended exposure to blue light levels of irradiation below threshold for thermal effects." (See Appendix B)

B. Burlington, Vt., Symposium on Light Damage, American Photobiology Society, June 1978, Invited Paper, W.T. Ham, "Sensitivity of the retina to radiation damage as a function of wavelength." (See Appendix D)

C. Meriden, N.H., Gordon Conference on Lasers in Medicine and Biology, J.J. Ruffolo in formal session, and J.J. Ruffolo, W.T. Ham, and A.M. Clarke each in a semiformal "Low light level" session described the MCV research.

8. Other Travel

A. San Francisco, Calif., LAIR: W.T. Ham, A.M. Clarke, H.A. Mueller, and J.J. Ruffolo to consult with Drs. Beatrice, Randolph, and Zwick at the USAJLST on the USAMRDC laser safety program.

B. Richmond, Va., MCV, April 1978: Maj. B. Reddington, Project Officer, Site visit with Dr. Ham, et al.

C. Richmond, Va., MCV, May 1978: Dr. Hocheimer and the Johns Hopkins medical photographer to discuss fundus photography with H.A. Mueller.

D. Edgewood Arsenal, Md., USAEHA, May 1978: A.M. Clarke and R.C. Williams to see D.H. Sliney to calibrate the MCV photodetector.

FIGURE LEGENDS

Figures 2-16 are electron micrographs of portions of a 2 day lesion (441 nm at 33 J/cm^2 for 1000 s) giving observations on the neural retina, pigment epithelium, and choroid.

2   Macrophage (MPh) between photoreceptor cells in the outer nuclear layer. X 11,600

3   Portion of a cone having dense cytoplasm. Cell junctions (CJ) appear normal (portion of Muller cell indicated by asterisk). The nature of the large vacuoles (v) in the cytoplasm of photoreceptor cells is uncertain (but see Figure 19). The basis of the denseness of the cone cytoplasm is also uncertain, but is likely due to glycogen granules (see Figure 19). X 29,000

4   Portion of RPE and choroid at low magnification. The choriocapillaris just below Bruch's membrane (BM) contains leucocytes including an eosinophil (E). The RPE cells are rounded and vacuolated. The melanosomes are disoriented and show stages of degeneration. Swelling of several outer segments at the top of the picture is probably an artifact of specimen preparation. X 5,500

5   Similar to Figure 4. X 5,500

6   Similar to Figure 4. Eosinophils (E) are readily recognized among the leucocytes in the choriocapillaris and choroid. X 5,500

7   Portion of RPE and choroid. RPE cells (a and b) are rounded, vacuolated, and raised off from Bruch's membrane (BM). They contain disoriented and degenerating melanosomes and lysosome-like bodies. A large portion of outer segment (OS) is seen next to Bruch's membrane. An eosinophil is apparent in the choriocapillaris. X 10,200

8   Damaged RPE cells. X 11,600

9   Part of RPE cell (PE) and subretinal space containing outer segments and membrane debris (thick arrow). A packet of discs is indicated by a curved arrow. In the RPE cell arrows indicate bundles of tubular membranes at low magnification. X 17,400

10   Portion of RPE cell showing degenerating melanosomes (mn) and some that have blanched spots (arrows). Longitudinal and cross sections of bundles of tubular membranes (btm) can be seen. Lysosome-like bodies (lys) are also apparent. X 29,000

11   Part of RPE cell showing bundles of tubular membranes (btm) in longitudinal section. X 49,300

12   Bundles of tubular membranes (btm) in an RPE cell. Cross sections can be seen at arrows. Numerous vesicles in the cytoplasm are apparent. X 49,300

-20-

13   Portion of choroid at low magnification showing parts of several melanocytes. A large aggregate of melanin in one of the melanocytes is indicated by an arrow. The curved arrow indicates a cell containing aggregates of melanosomes. An eosinophil (E) is evident. X 6,000

14   Portion of choroid showing melanocytes and numerous leucocytes, including an eosinophil (E) and an apparent macrophage (MPh). The curved arrow indicates a cell with digestive vacuoles containing very dense melanin granules and a homogeneous dense matrix. X 5,500

15   Probable macrophage (MPh) in the choroid. Digestive vacuoles (arrows) are seen at higher magnification. X 14,500

16   Melanocytes (M) and probably macrophage (MPh) in the choroid. Several melanosomes have blanched spots. X 14,500

Figures 17-30 are electron micrographs of portions of a 5 day lesion (435 nm at 35 J/cm^2 for 1000 s) giving observations on the neural retina, pigment epithelium, and choroid.

17   Synaptic zone of the outer plexiform layer showing a macrophage (MPh). X 16,800

18   Portion of the outer plexiform layer next to the outer nuclear layer showing a macrophage containing a lysosome-like body (lys). X 34,800

19   Part of a dense cone (lower) and a rod cell (upper) inner segment with a Muller cell process (asterisk) between them. A swollen mitochondrion (mit) is evident as well as vacuoles (v). Since many cisternae of the rough endoplasmic reticulum (rer) are somewhat swollen, it is likely that the larger vacuoles are distended cisternae. The denseness of the cone cytoplasm is due in large part to particles (probably glycogen; indicated by arrowheads) larger than bound (rer) and free ribosomes (arrows). X 45,000

20   A cone ellipsoid showing an array of tubular membranes (tm), vesicles (v), and disc-like membranes (dm). X 23,200

21   Similar to Figure 20, showing tubular (tm) and disc-like (dm) membranes in a cone ellipsoid. X 29,000

22   A macrophage (MPh) in the subretinal space containing a wide variety of debris and residuum including melanosomes (mn) and lipid-like bodies (L). X 16,800

23   RPE cells and a macrophage (MPh) in the subretinal space, having a well-developed Golgi complex (curved arrow) and phagocytized material such as a piece of outer segment (OS) and melanosomes (mn). The RPE cells lack malanosomes, but for lysosome-like bodies that appear to contain melanin. Mitochondria (mit) are swollen, and a Golgi complex (GC) and cell junction (arrow) are indicated. X 12,000

24   RPE cells and macrophages (MPh) in the subretinal space. The cytoplasm of an RPE cell shows both rough (rer) and smooth (ser) endoplasmic reticulum and a Golgi complex (curved arrow), as well as lysosome-like (lys) and lipid-like (L) bodies. Vacuoles (v) appear to be swollen mitochondria. X 15,000

25   RPE cells (a and b) showing a Golgi complex (curved arrow), smooth endoplasmic reticulum (SER), swollen mitochondria (mit), melanosomes (mn), and a dense flocculent material (F). X 24,000

26   RPE cells showing interdigitation next to Bruch's membrane (BM) and a cell junction (CJ) between a large cell profile and a finger-like cell process. Among the cytoplasmic inclusions are disc-like membranes (dm), a myelin-like figure (arrow), and dense flocculent material (F). X 14,500

27   RPE cells showing melanosomes having blanched spots (arrows) and strange ribbon or bar-like objects (box). X 24,000

28   RPE cell cytoplasm showing fuzzy ribbons (curved arrow) at higher magnification and dense flocculent material (F). X 45,000

29   Eosinophil (E) and part of a melanocyte (M) in the choroid. Several melanosomes have blanched spots. X 22,400

30   Apparent macrophage (or autophagous melanocyte) with degenerating melanosomes. Several melanosomes (arrows) have blanched spots. X 24,000

Figures 31-45 are electron micrographs of portions of a 6 day lesion (441 nm at 33 J/cm^2 for 1000 s) giving observations on the neural retina, pigment epithelium, and choroid.

31   Portion of a cone inner (IS) and outer (OS) segment. The OS shows a variety of membrane configurations. X 14,500

32   Cone OS at higher magnification to show disc-like (dm) and tubular (tm) membrane configurations. Numerous vesicular profiles are also evident. A multivesicular body is indicated by the arrow. X 23,200

33   A macrophage in the subretinal space containing a piece of outer segment (OS) and melanosomes, some of which have blanched spots (arrows). X 17,400

34   A macrophage (MPh) in the RPE near Bruch's membrane (BM). The cytoplasm contains lipid-like bodies (L), and several melanosomes have blanched spots (arrows). X 14,500

35   RPE cells showing considerable interdigitation and some attachments (arrows). Part of a macrophage is seen at upper left. X 11,600

36   RPE cells well-aligned on Bruch's membrane (BM) contain little or no melanin. Well-developed Golgi complexes (GC) and cell junctions (CJ) are indicated. Part of a macrophage in the subretinal space can be seen at upper right. X 14,500

37   RPE cells showing Golgi complexes (GC) and smooth endoplasmic reticulum (ser). The upper cell has several lysosome-like bodies that appear to contain melanin. X 11,600

38   RPE cells showing a cell junction (CJ), Golgi complex (GC), and cytoplasmic filaments (arrows). Bruch's membrane is at lower left. X 23,200

39   Melanocytes and apparent macrophage (center) in the choroid. Large digestive vacuoles containing melanosomes and a dense matrix are indicated by arrows. X 14,500

40   A large digestive vacuole (arrow) at higher magnification. Below are parts of melanocytes, and their melanosomes show frequent blanched spots. X 23,200

41   Melanocytes in which both individual melanosomes and large clumps of melanin have numerous blanched spots. X 29,000

42   Parts of melanocyte (upper) and macrophage (lower) in the choroid. Membrane-lipid bodies (arrows) are seen in this macrophage. Melanosomes in digestive vacuoles (below) and in the melanocyte (above) have blanched spots. X 29,000

43   Part of a melanocyte showing melanosomes at higher magnification. Numerous blanched spots are evident.   X 34,800

44   Similar to Figure 43, showing blanched spots in melanosomes. X 43,500

45   Similar to Figure 43, showing melanosomes at higher magnification. Microfibrils in the melanocyte cytoplasm are apparent.   X 58,000

26
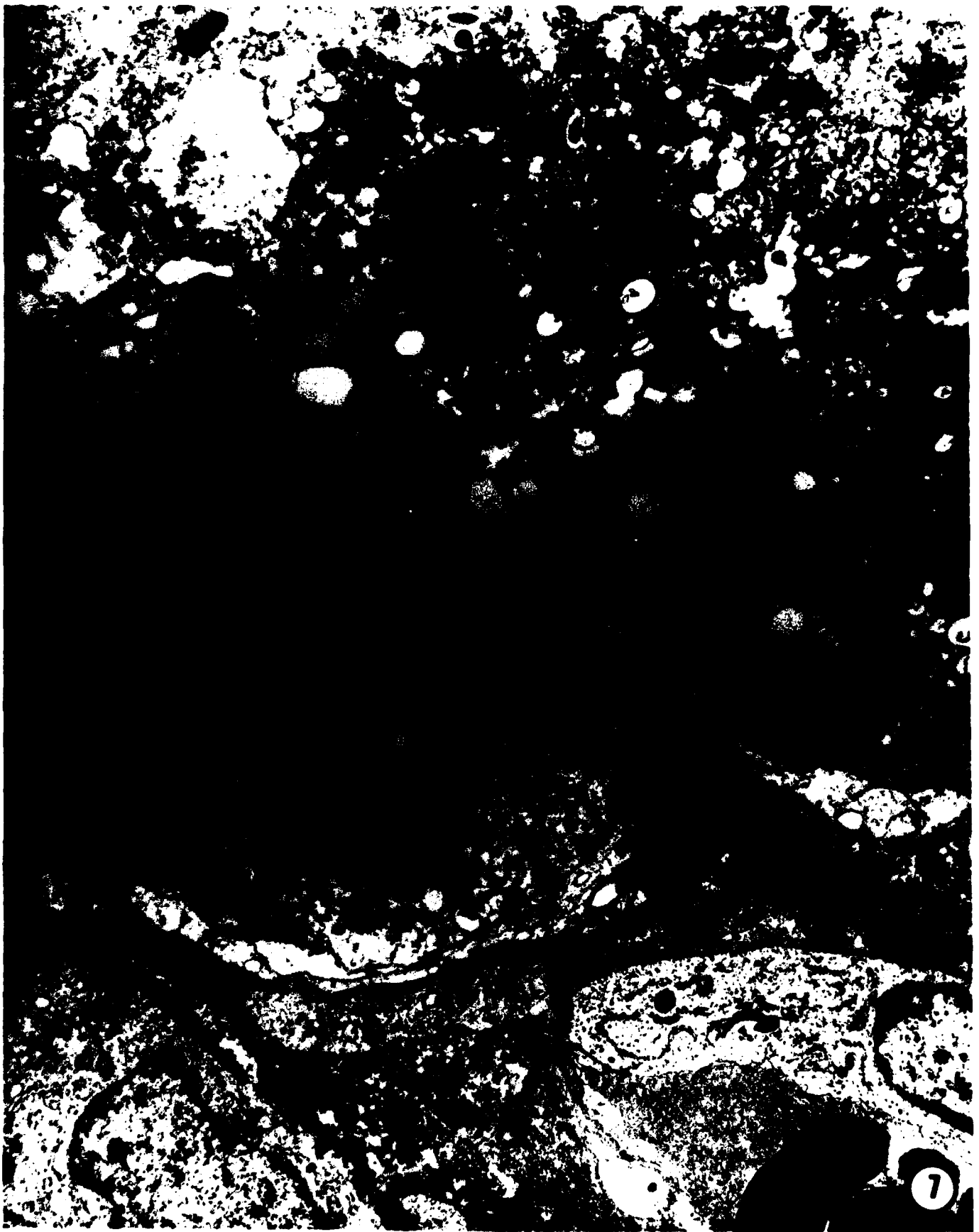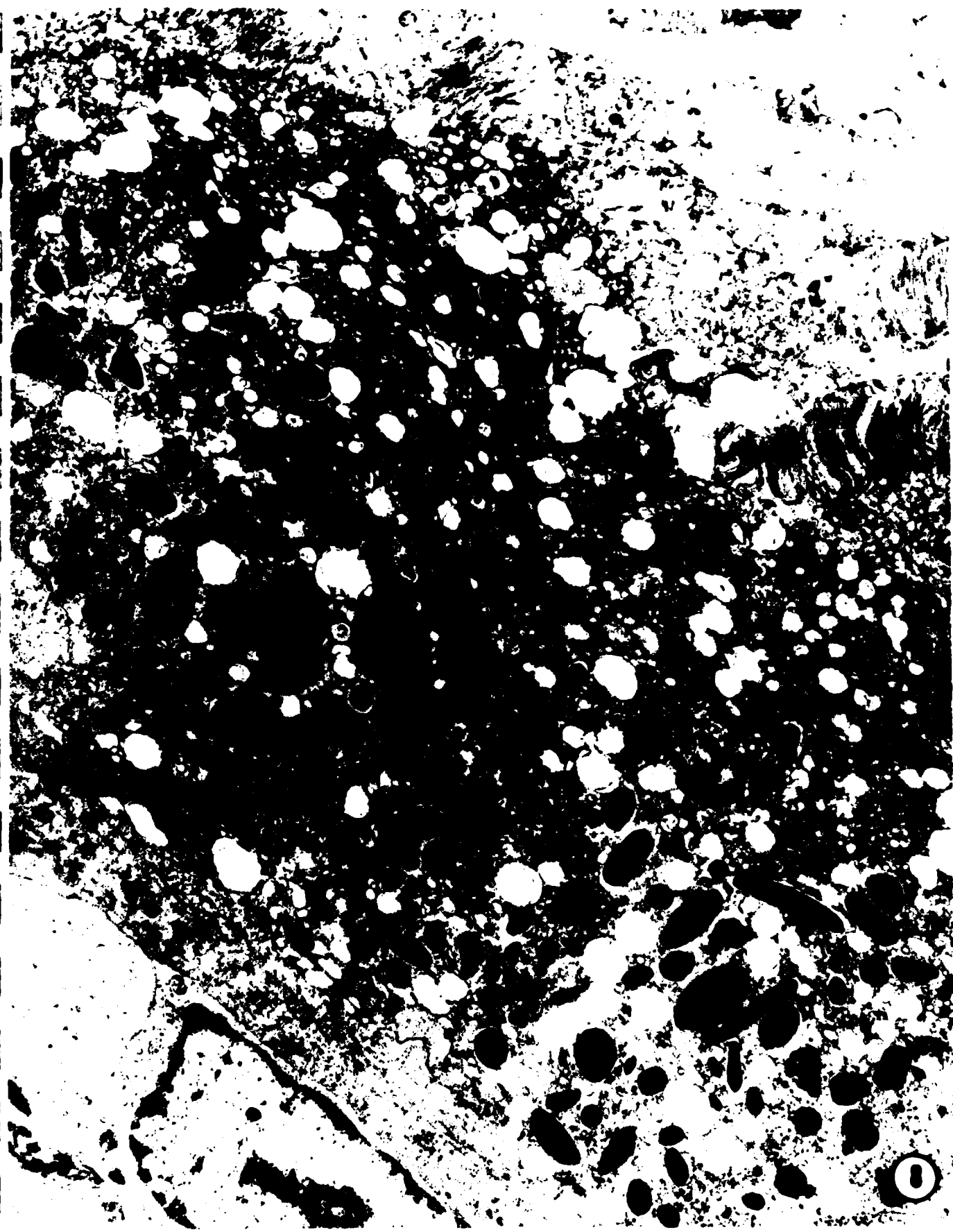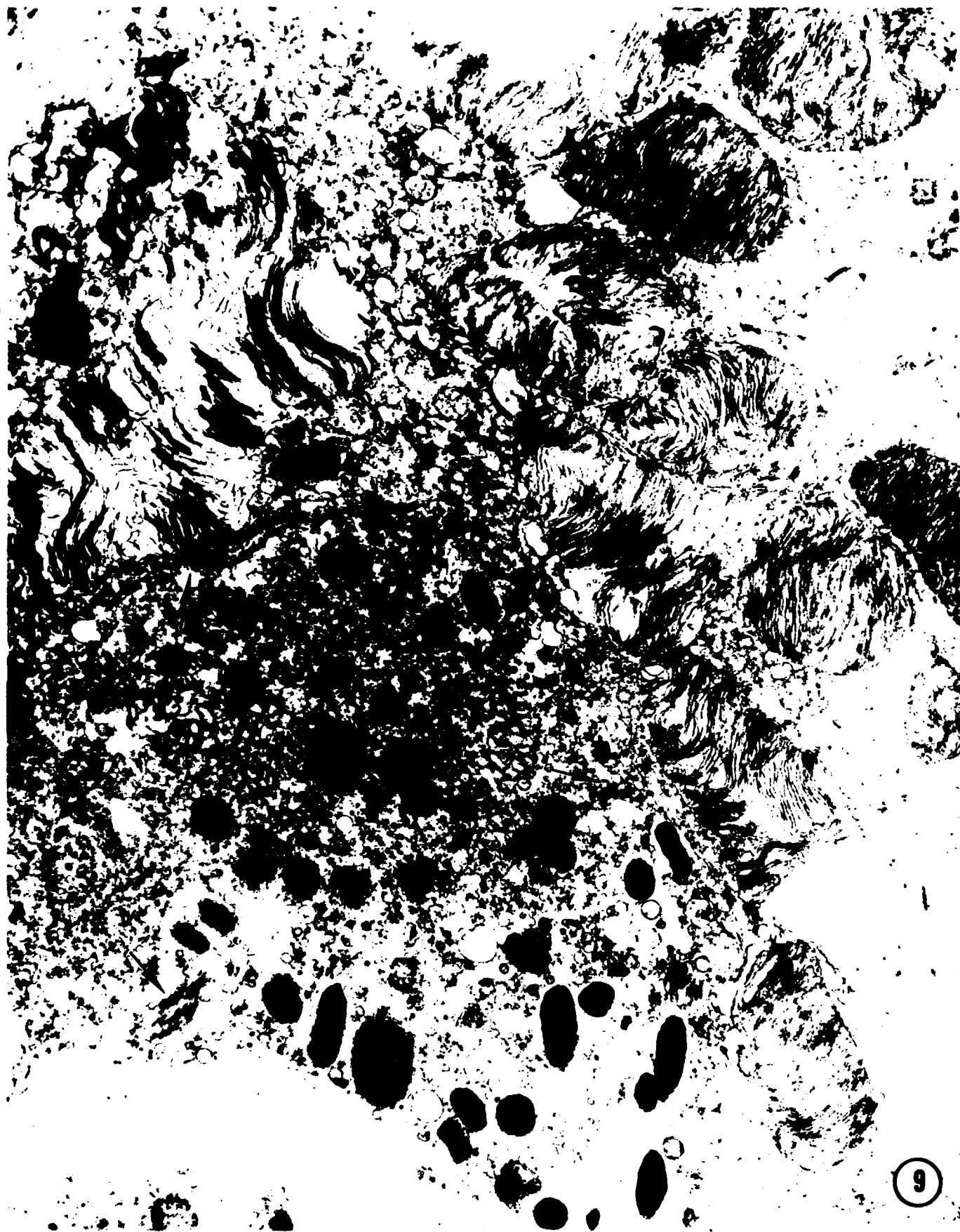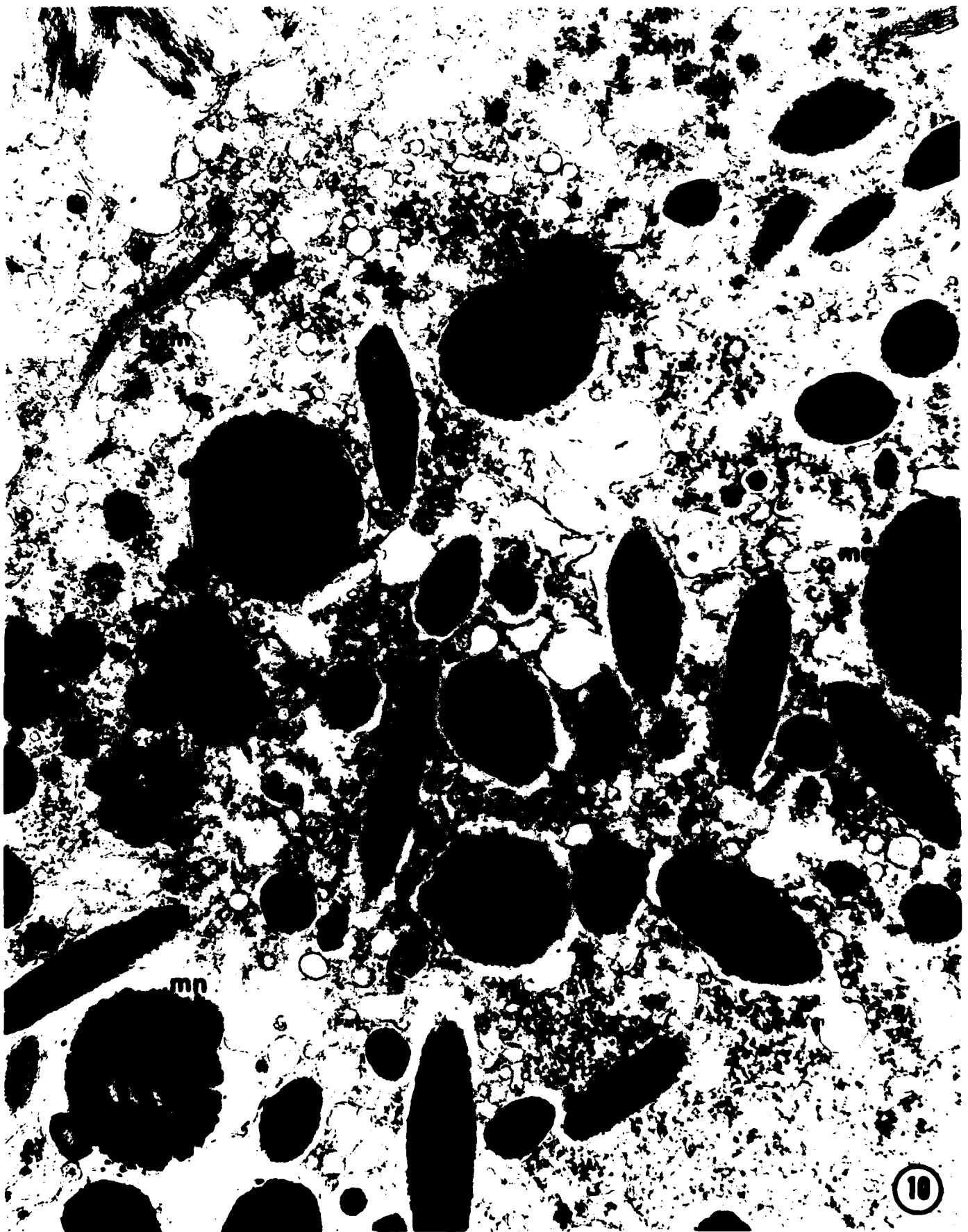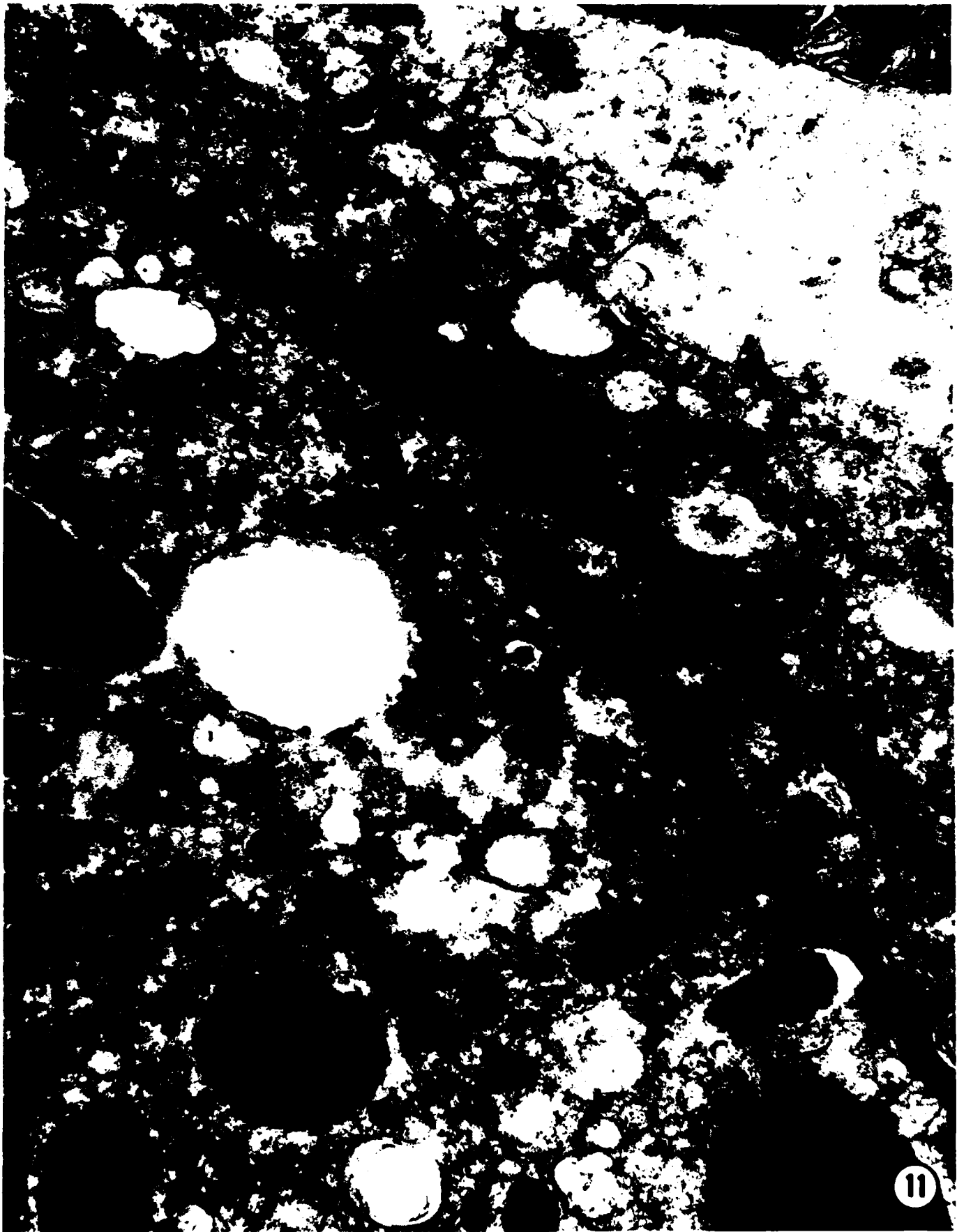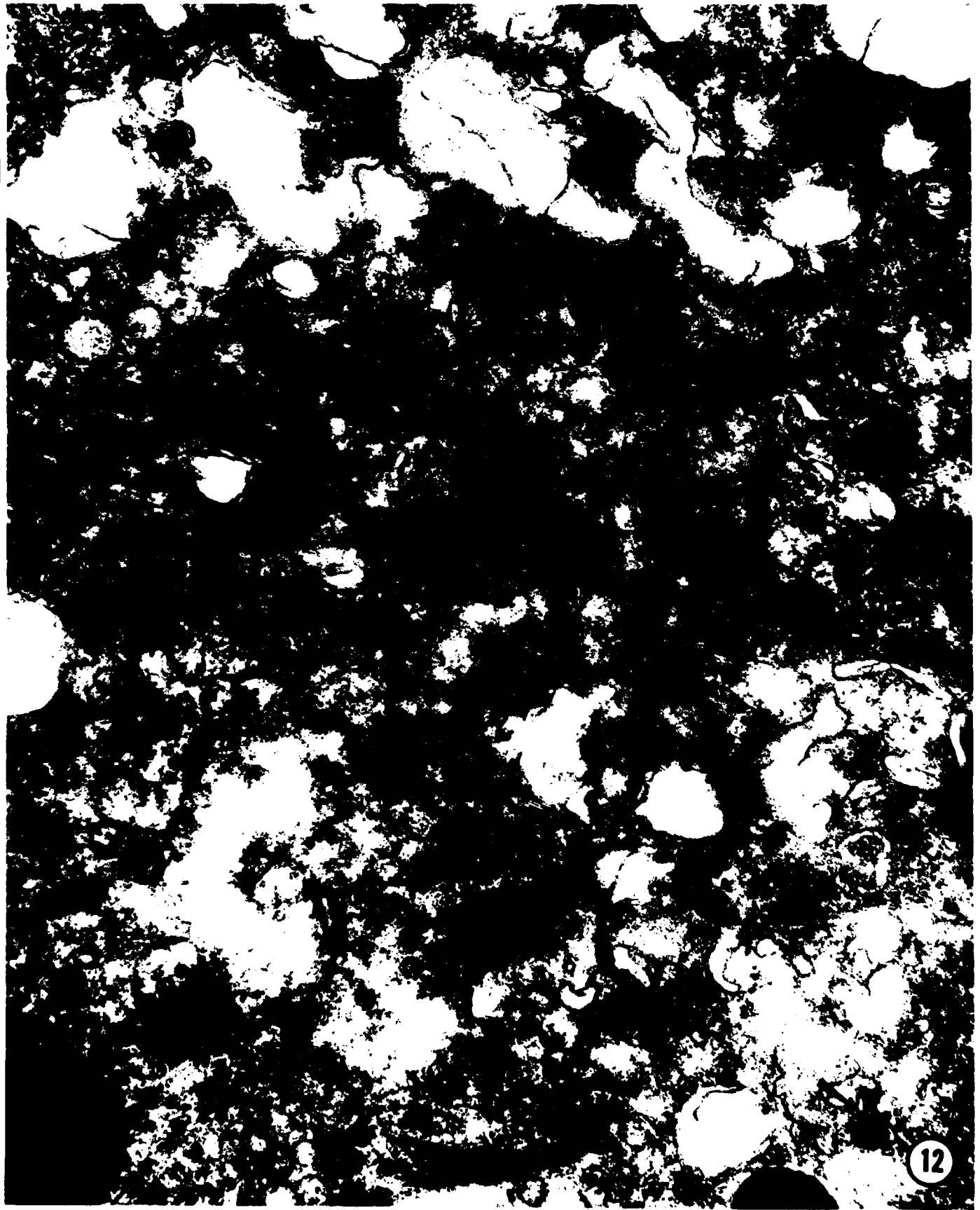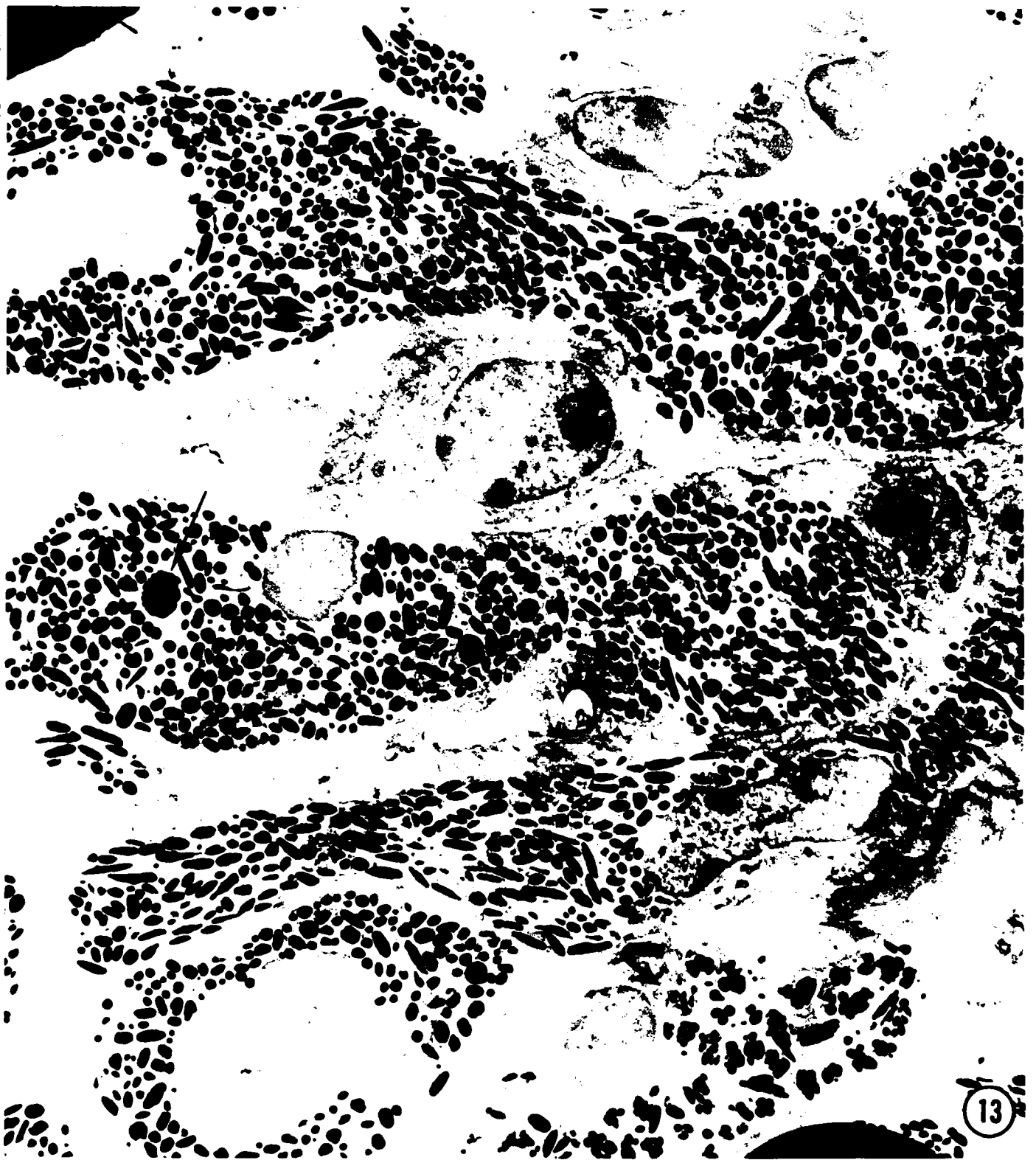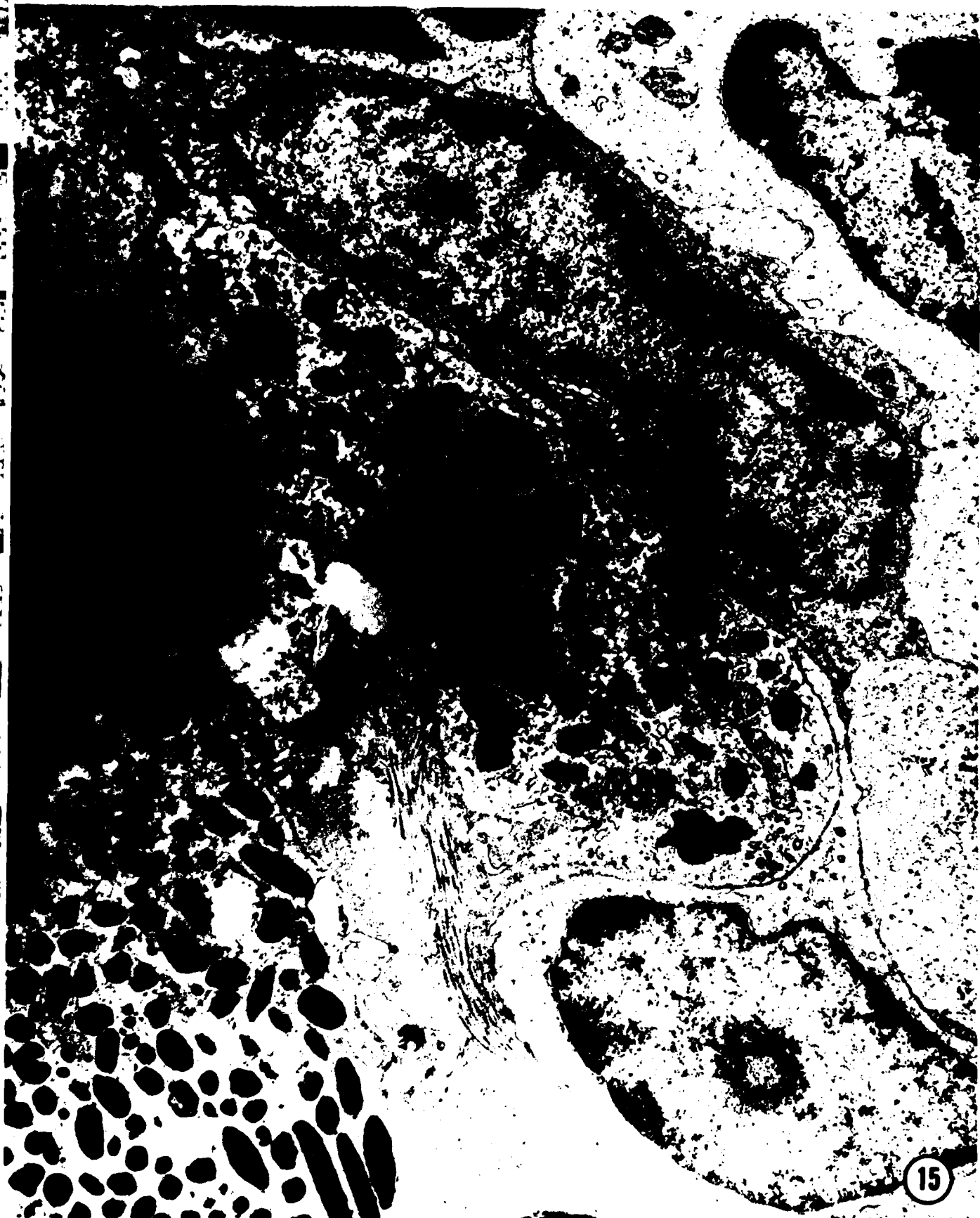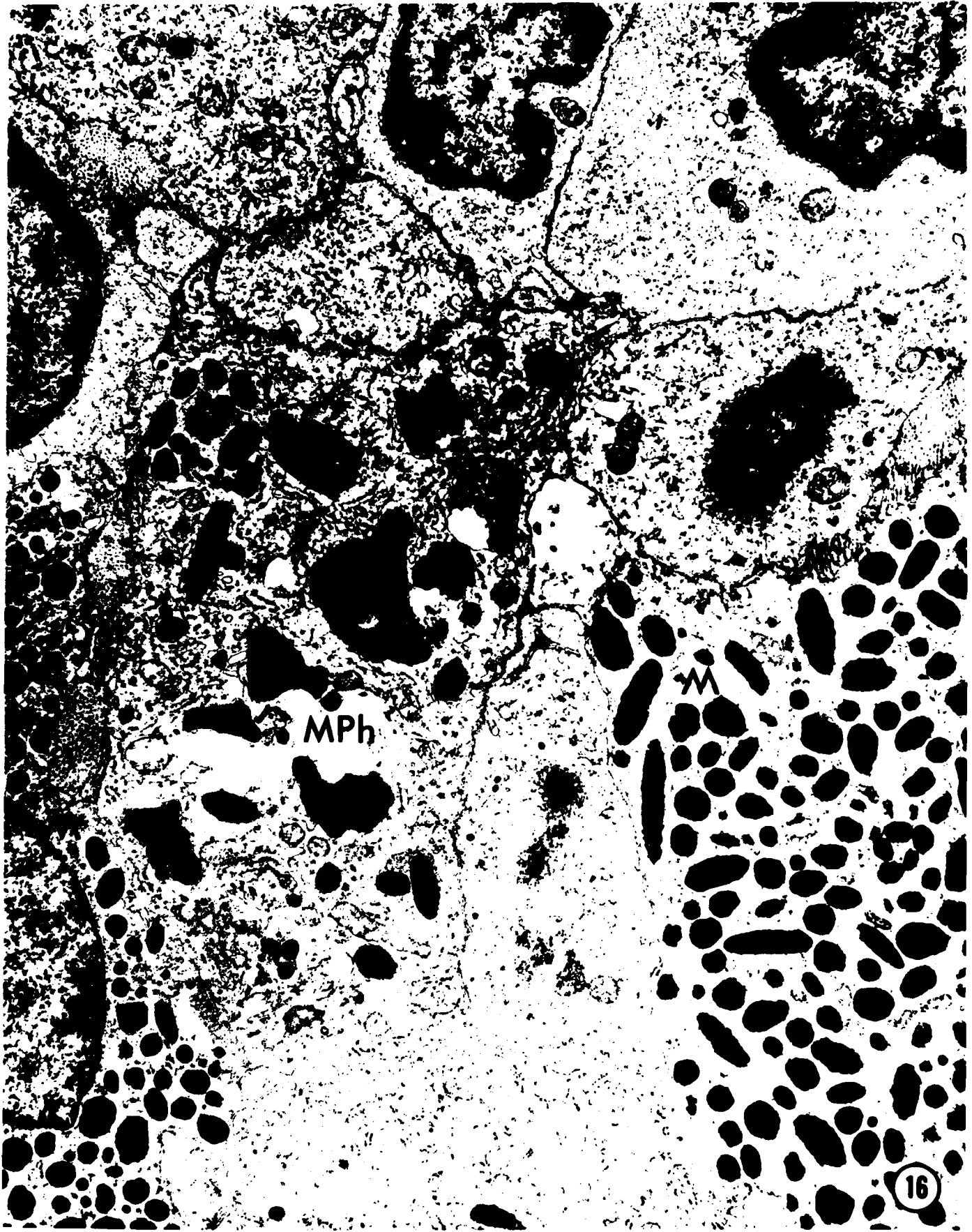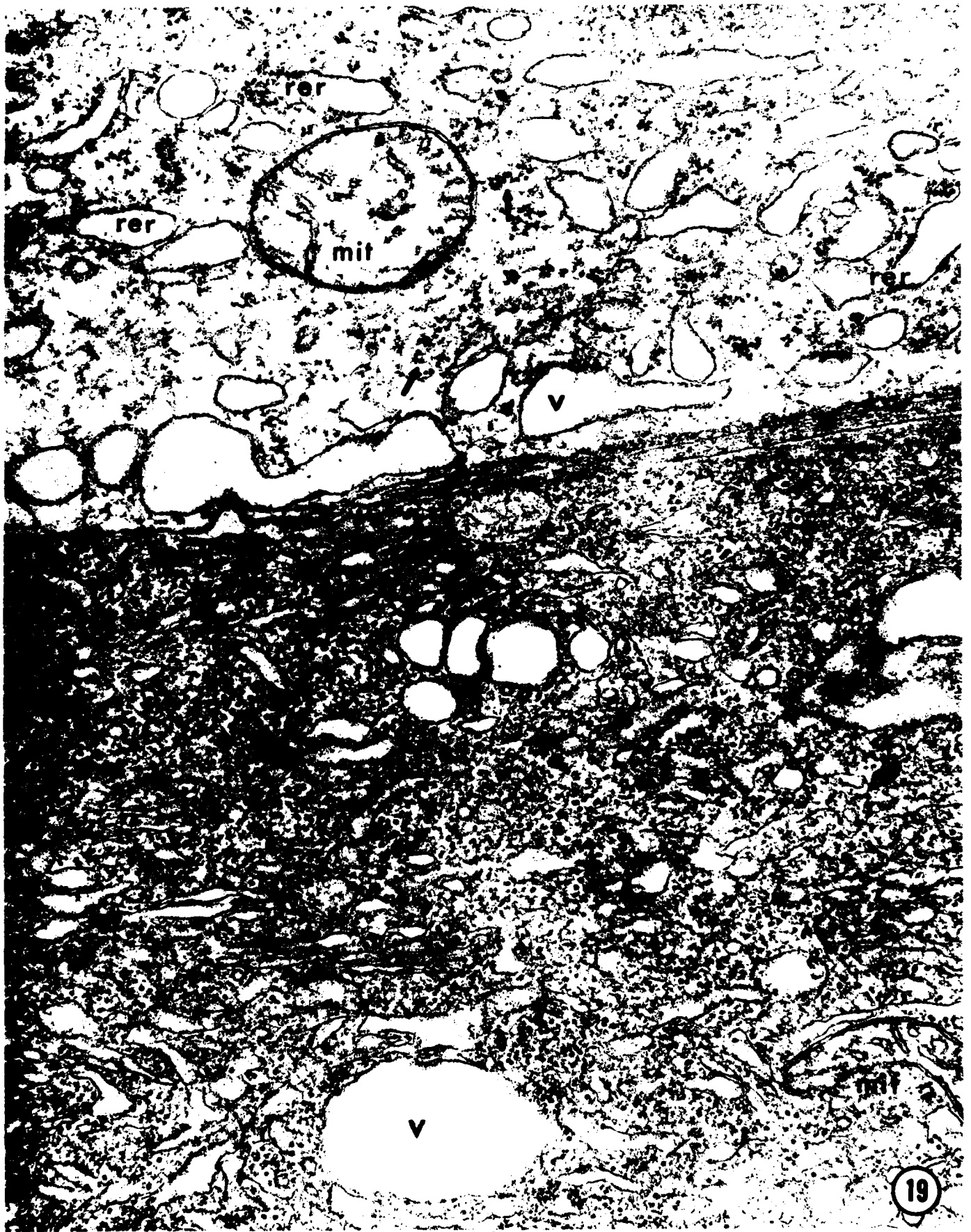
27

28

30

32

33

9

mp

mp

34

⑩

35

MPh

M

16

40

Mph

⑰

41

lys

18

42

rer

rer

mit

rer

v

v

mit

43

19

mit

20

22

mn

OS

23

47

MPh

V

V

48

24
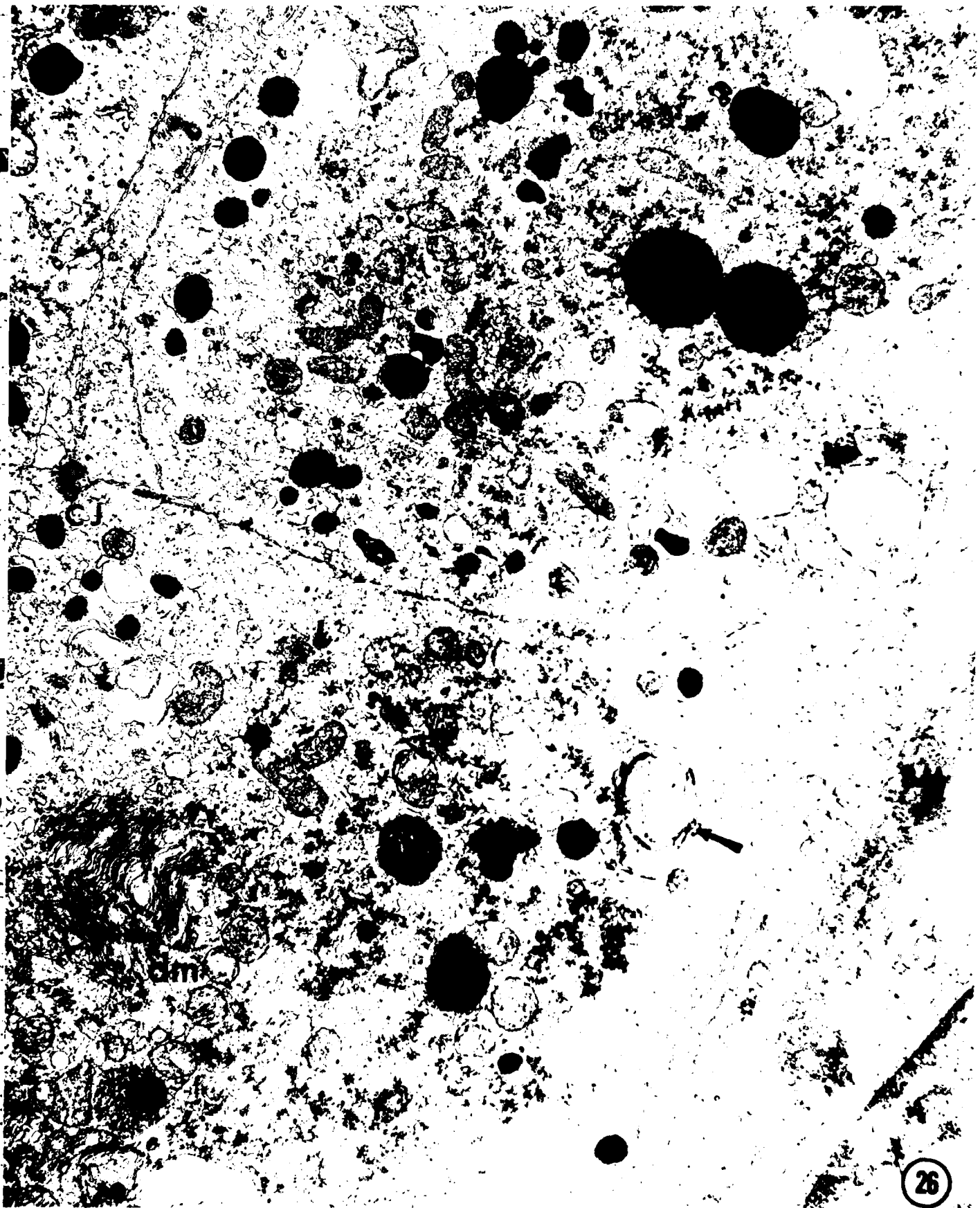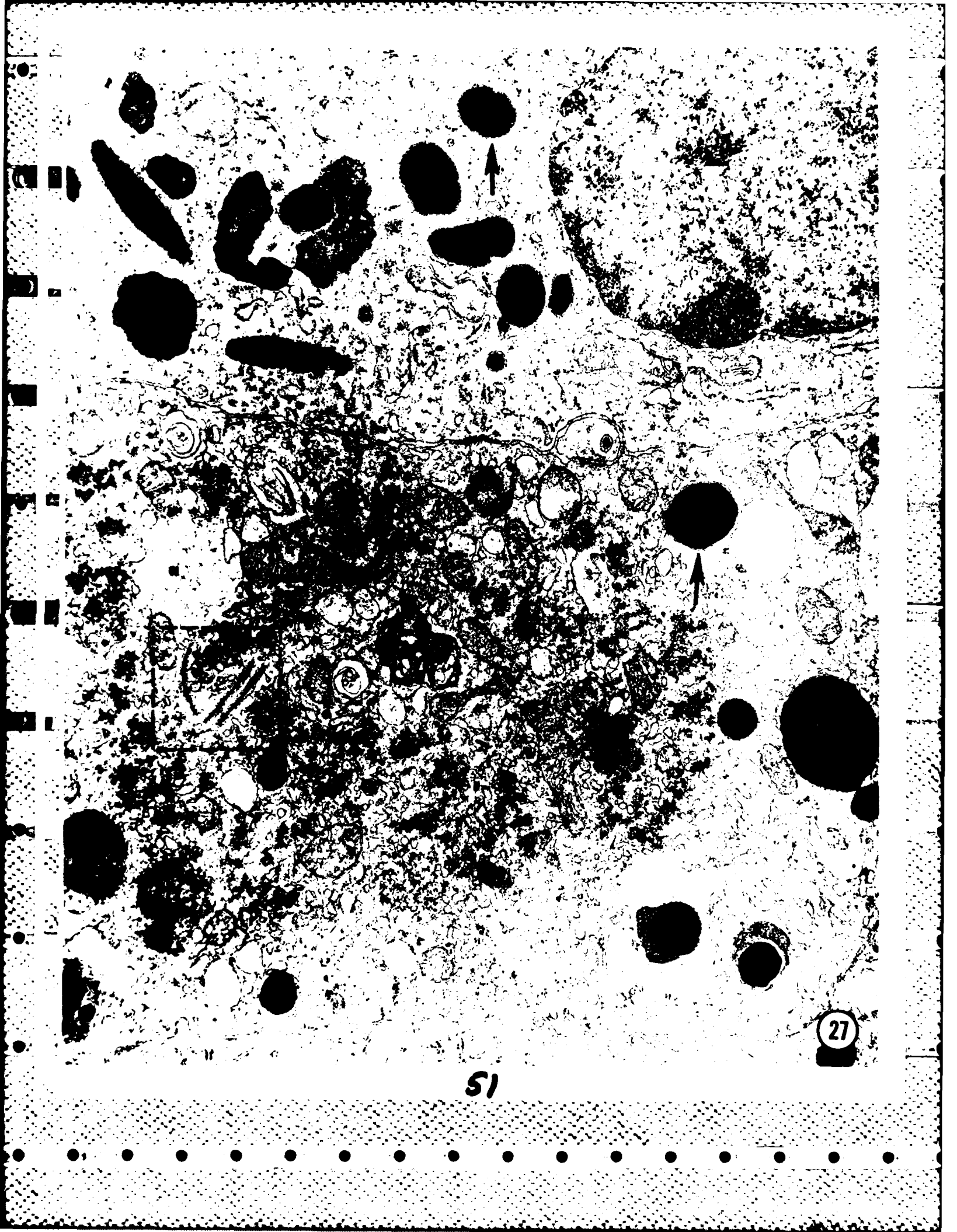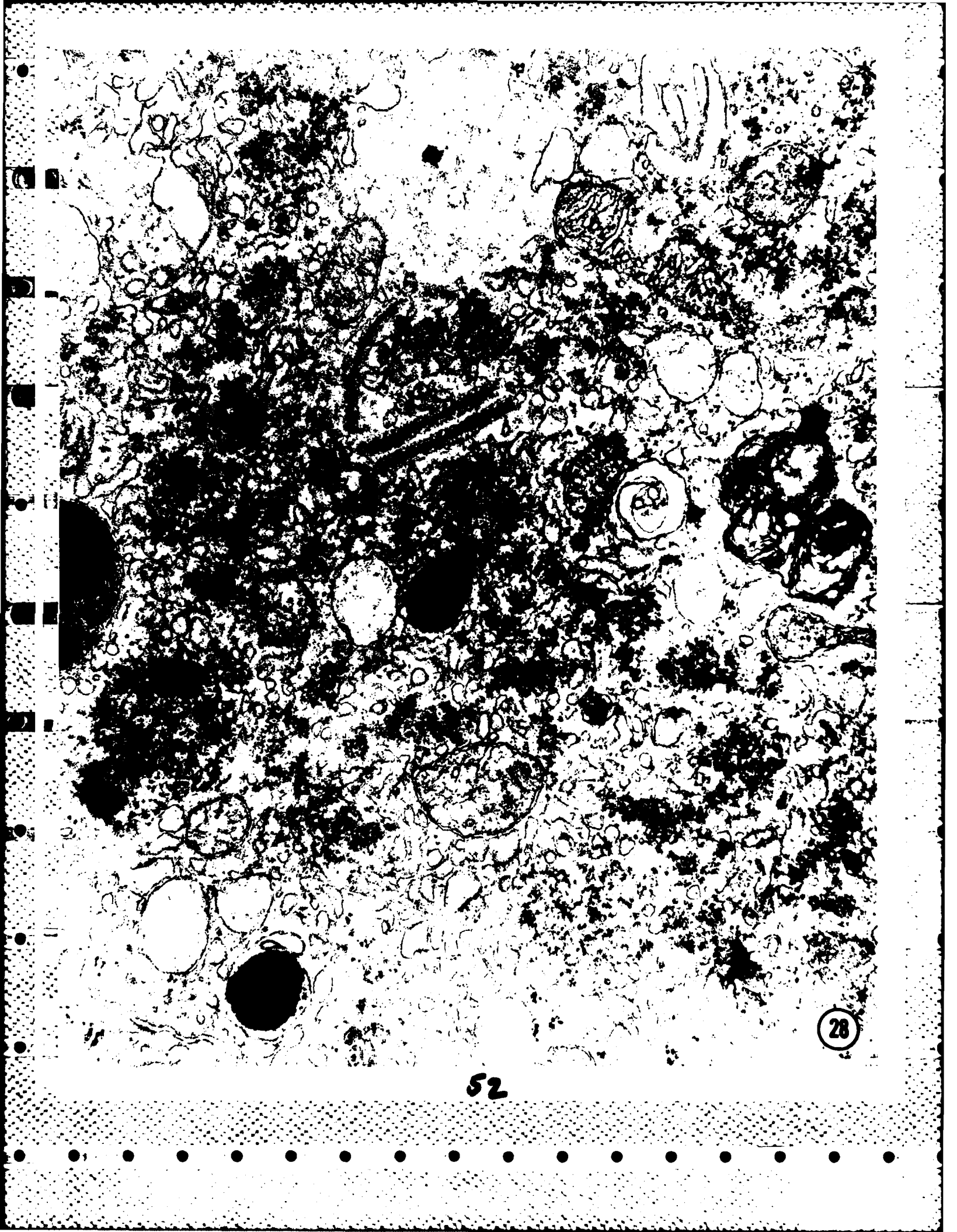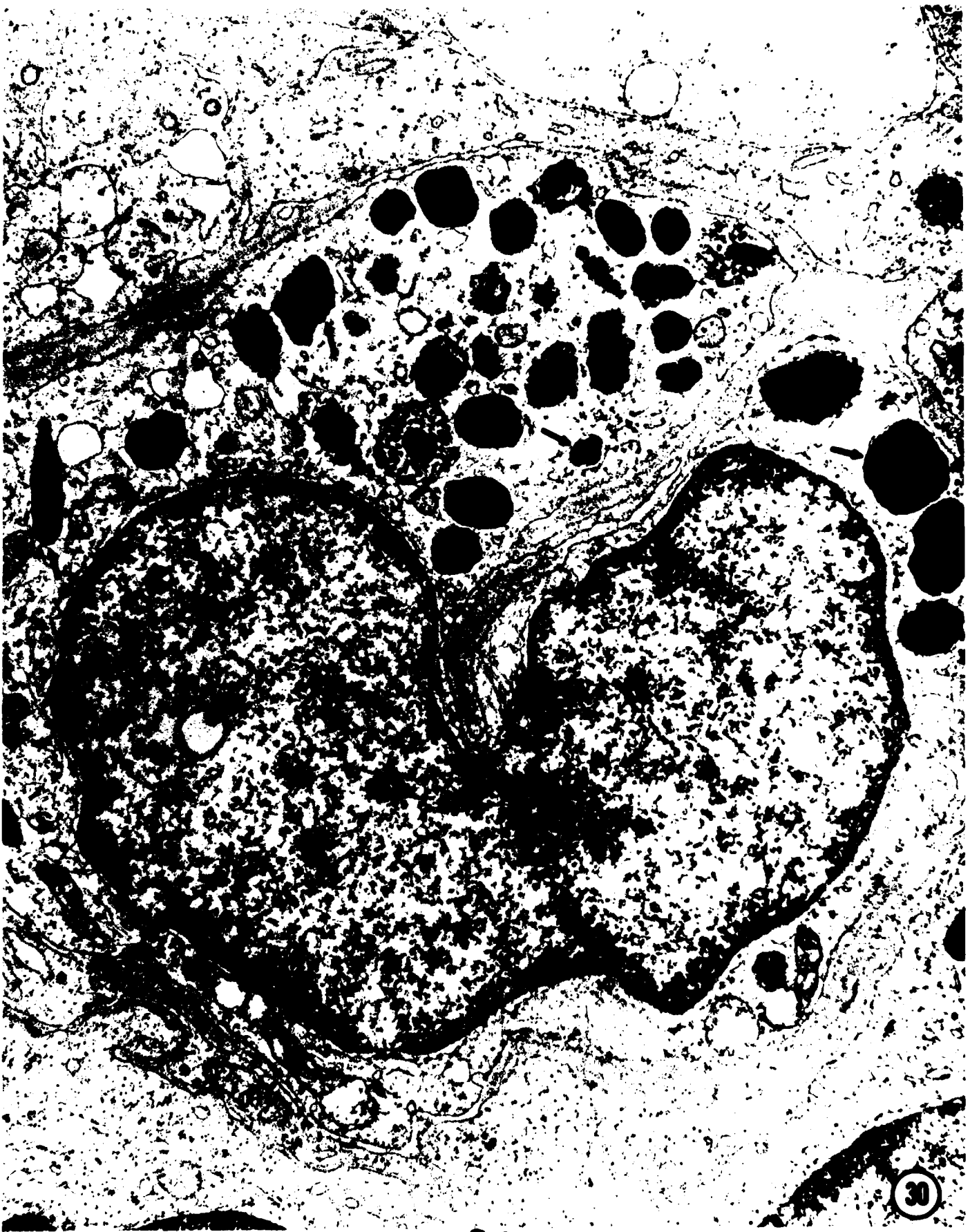
cj

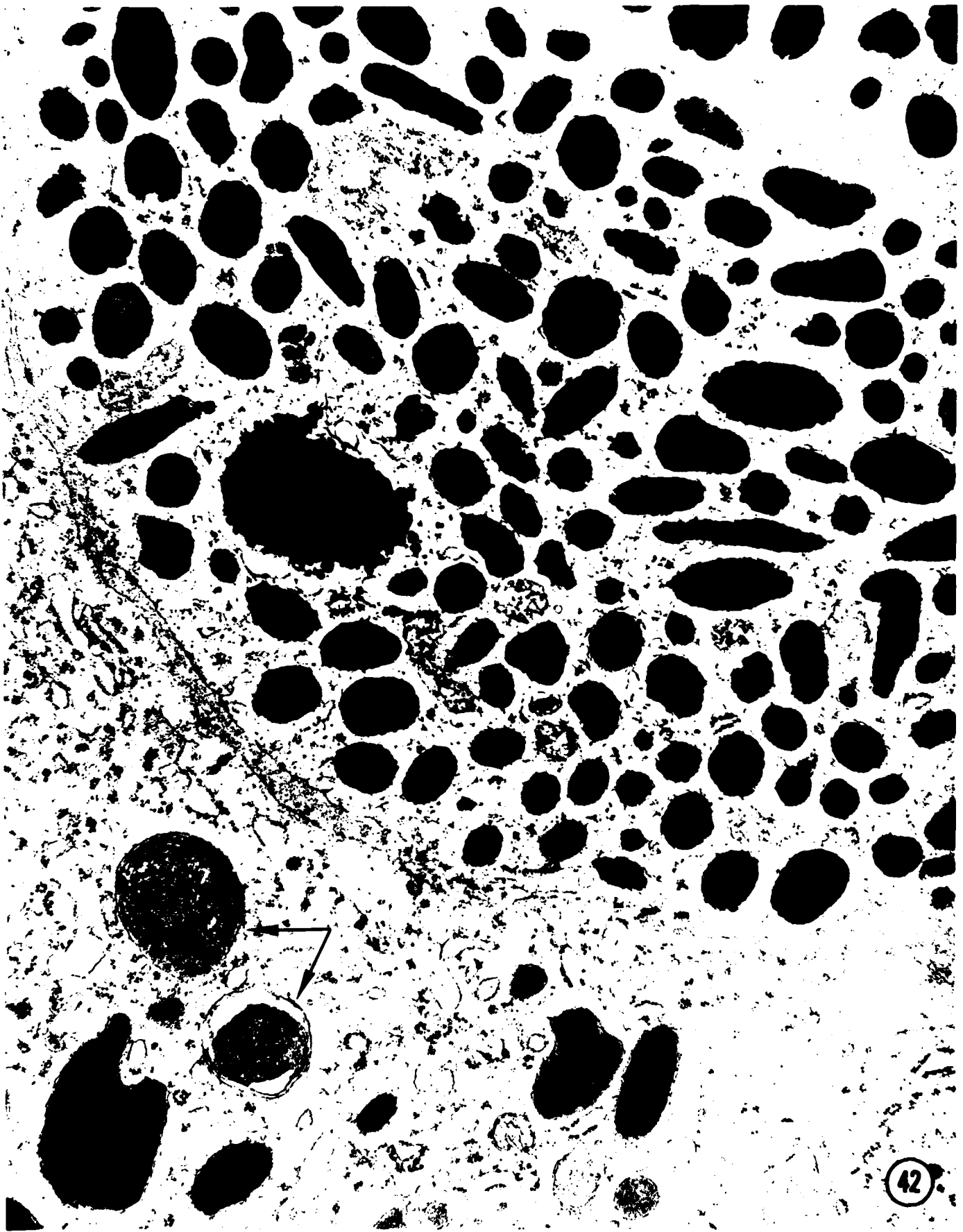dm

50

26

51

27

52

28

57

33

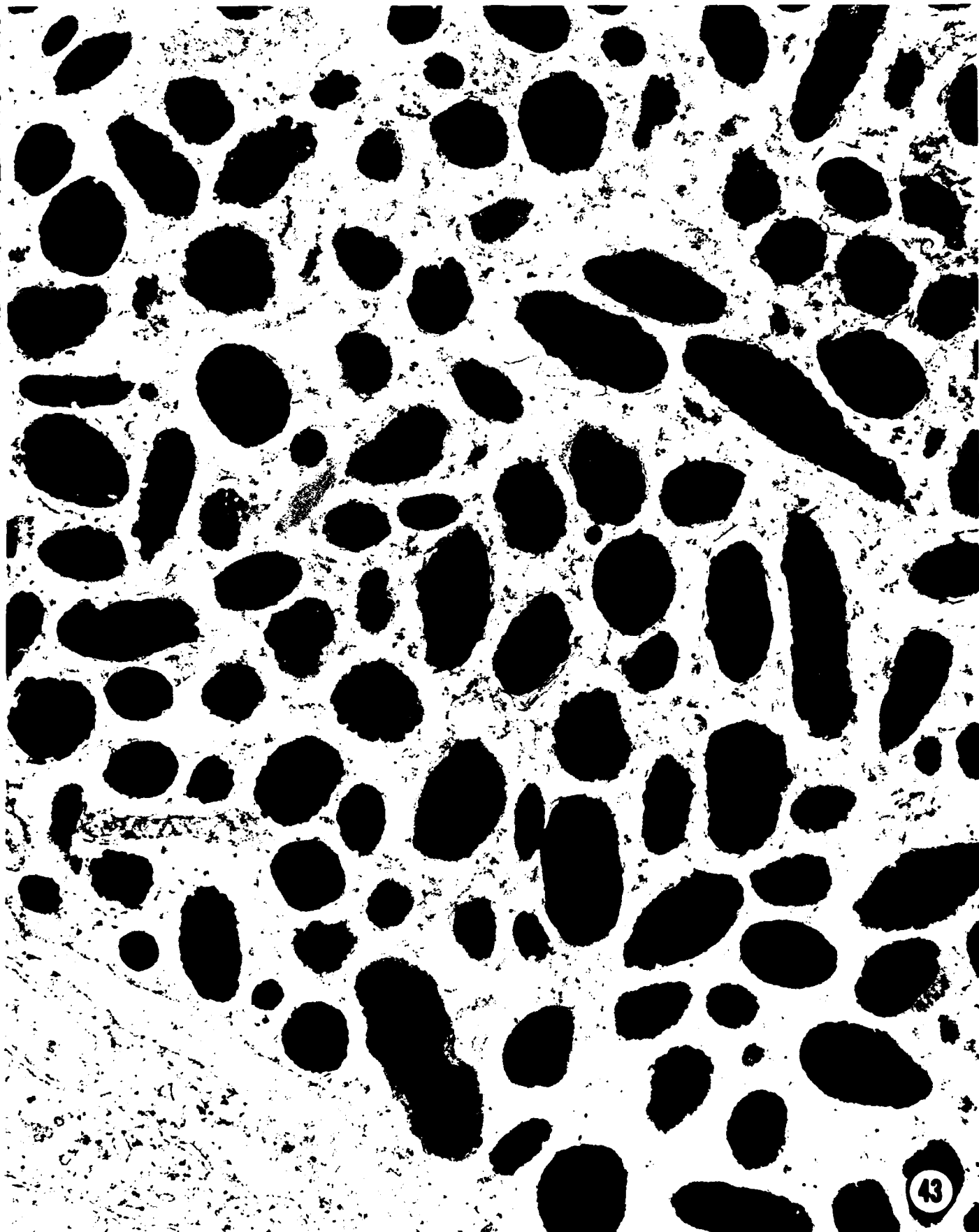58

34

35

CJ

GC

60

36

62

38

63

39

64

40

65

41
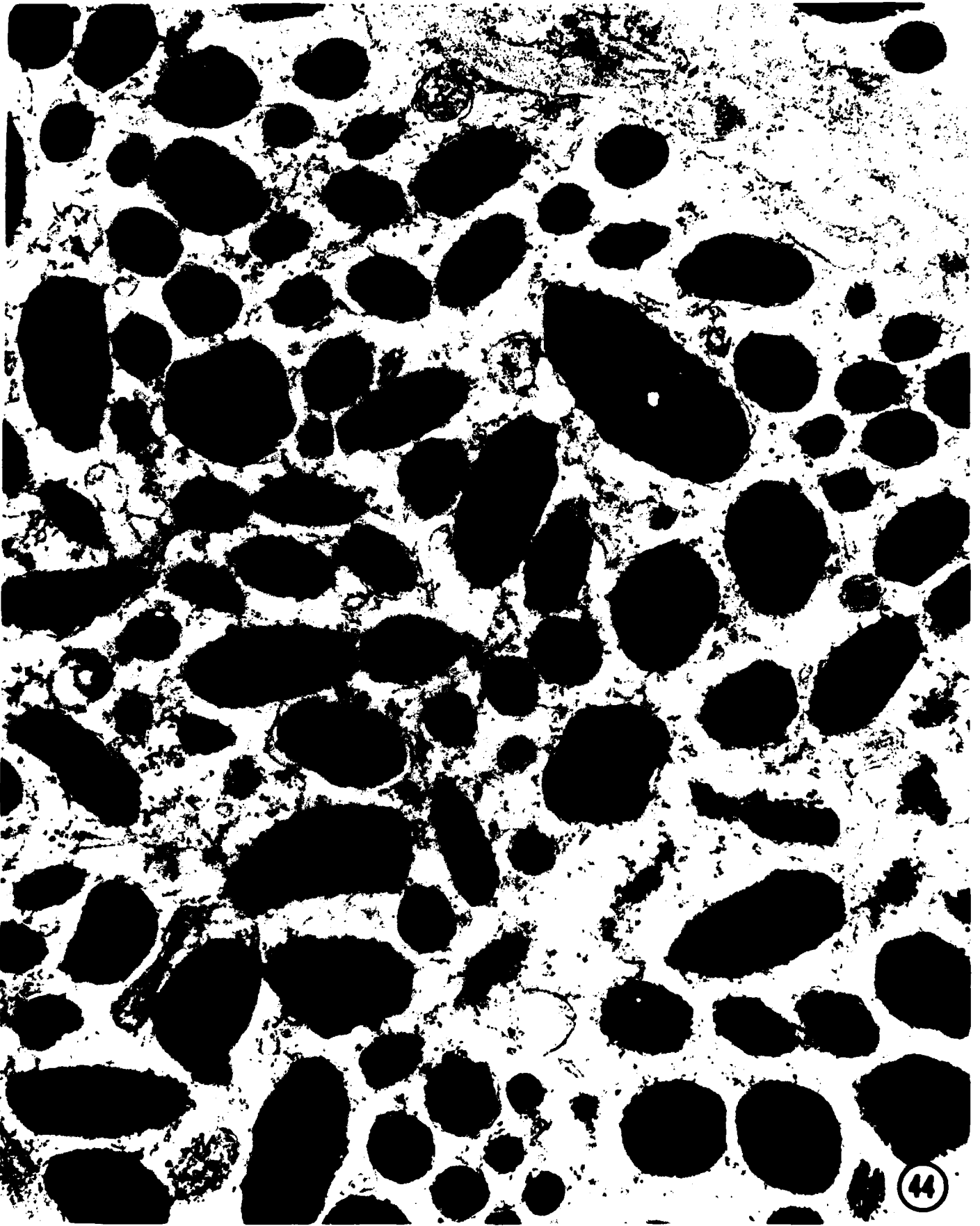
42
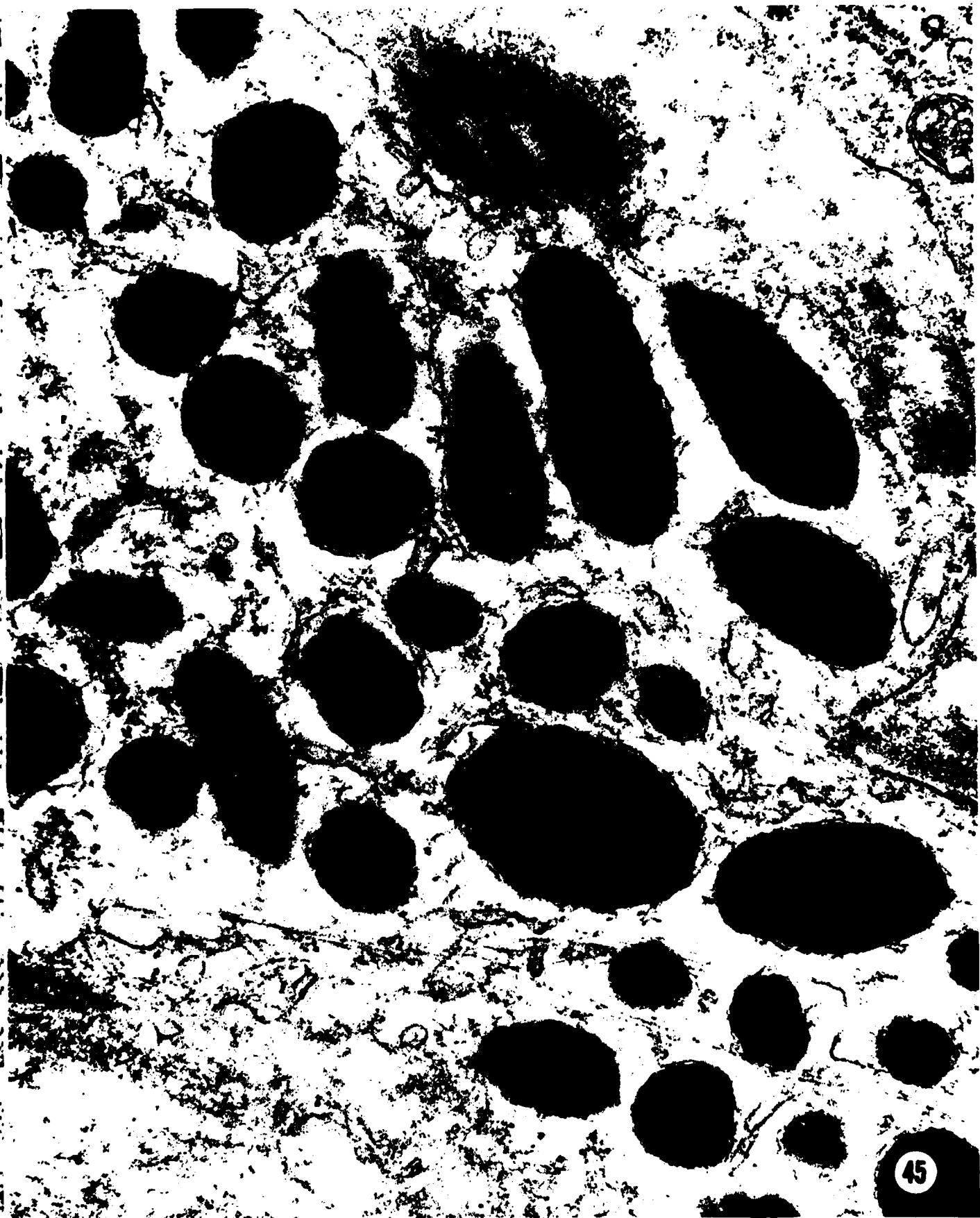
67

43

68

45
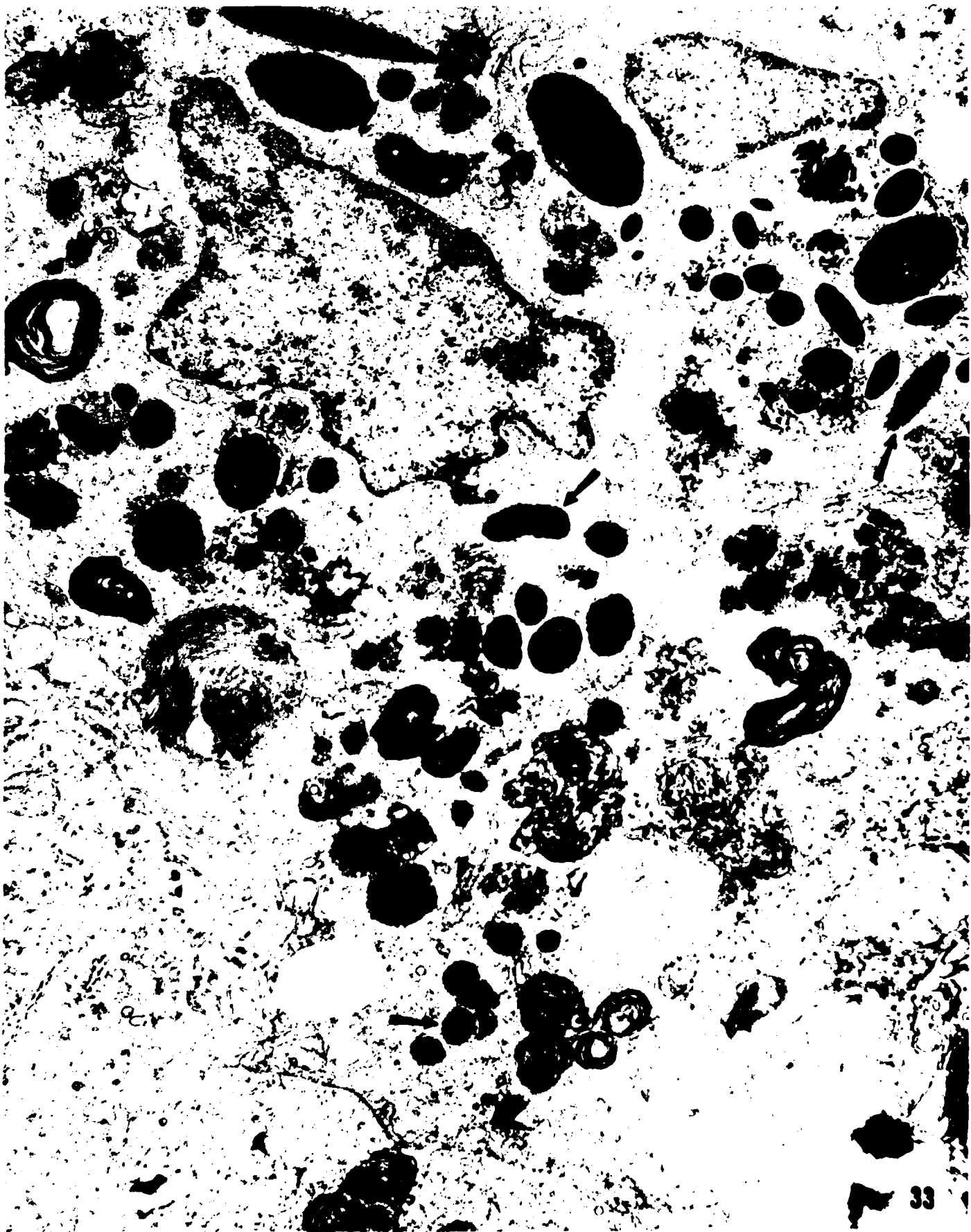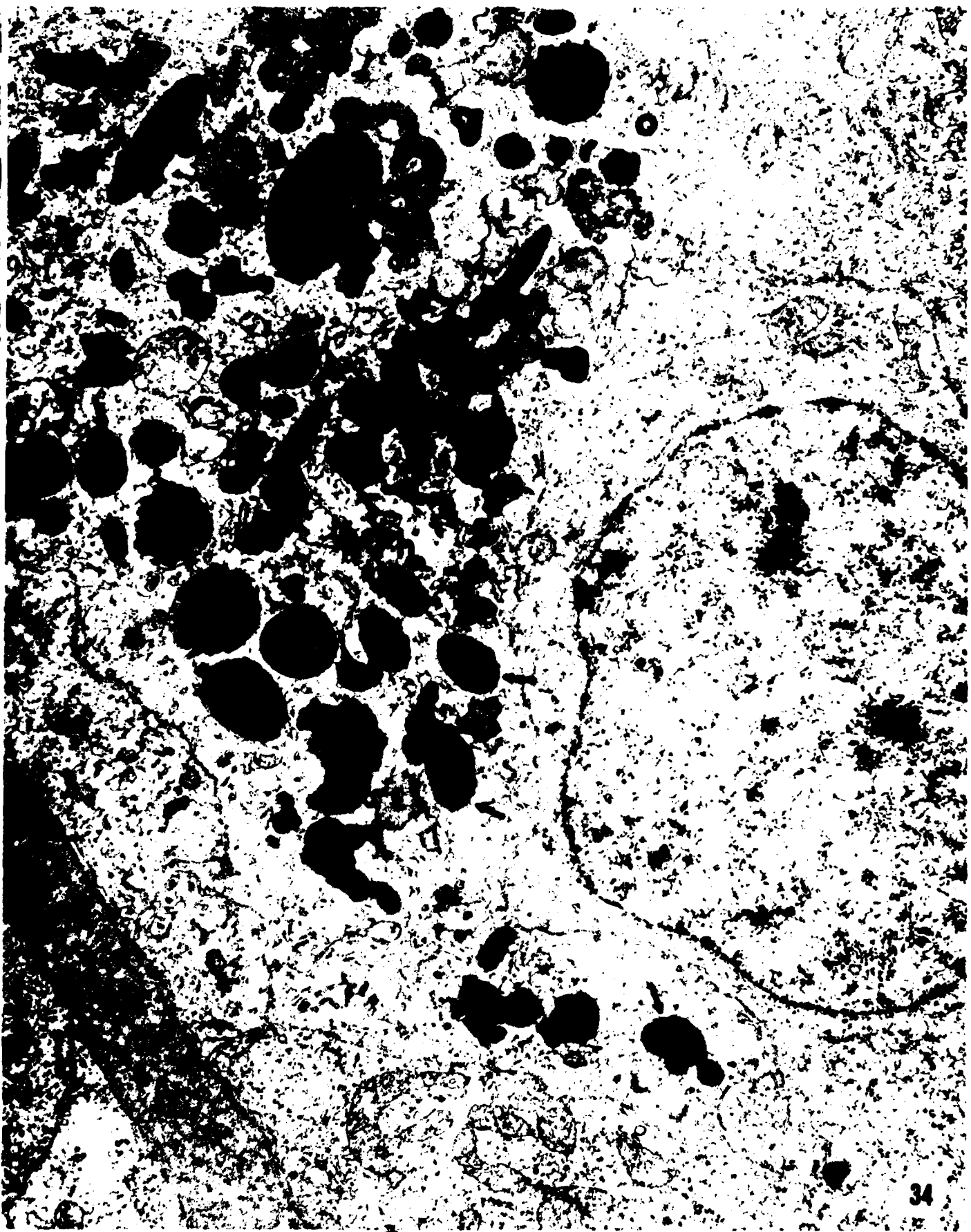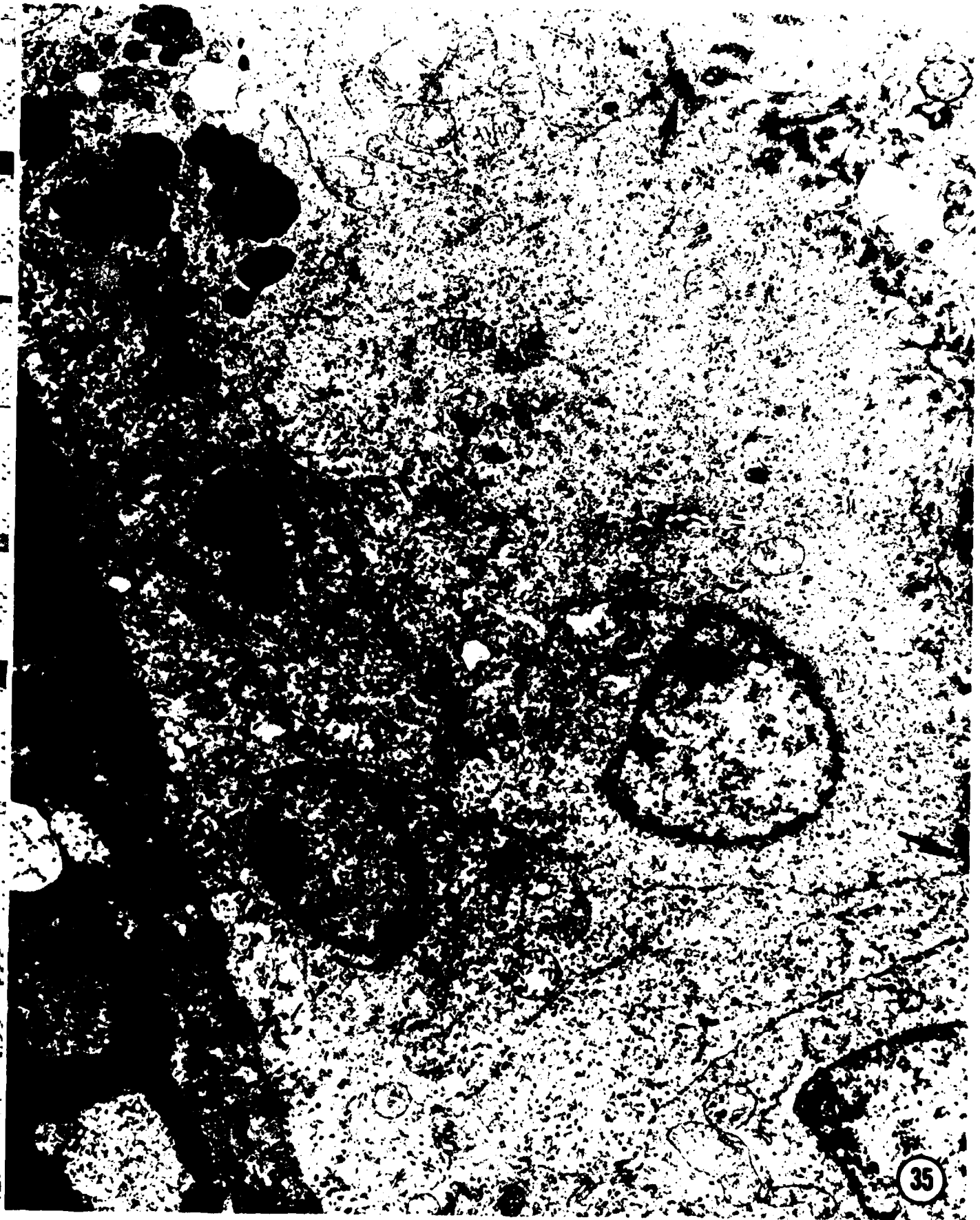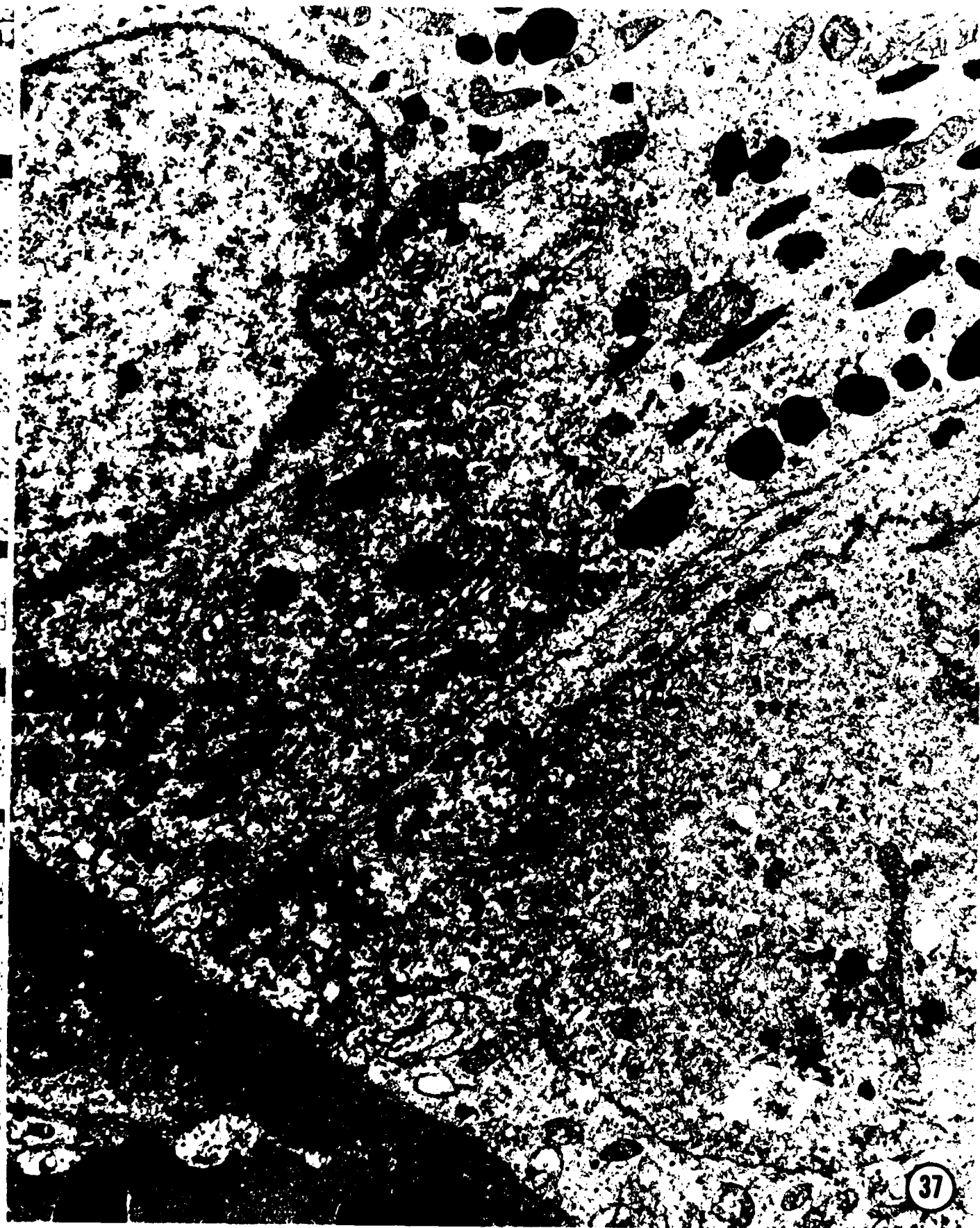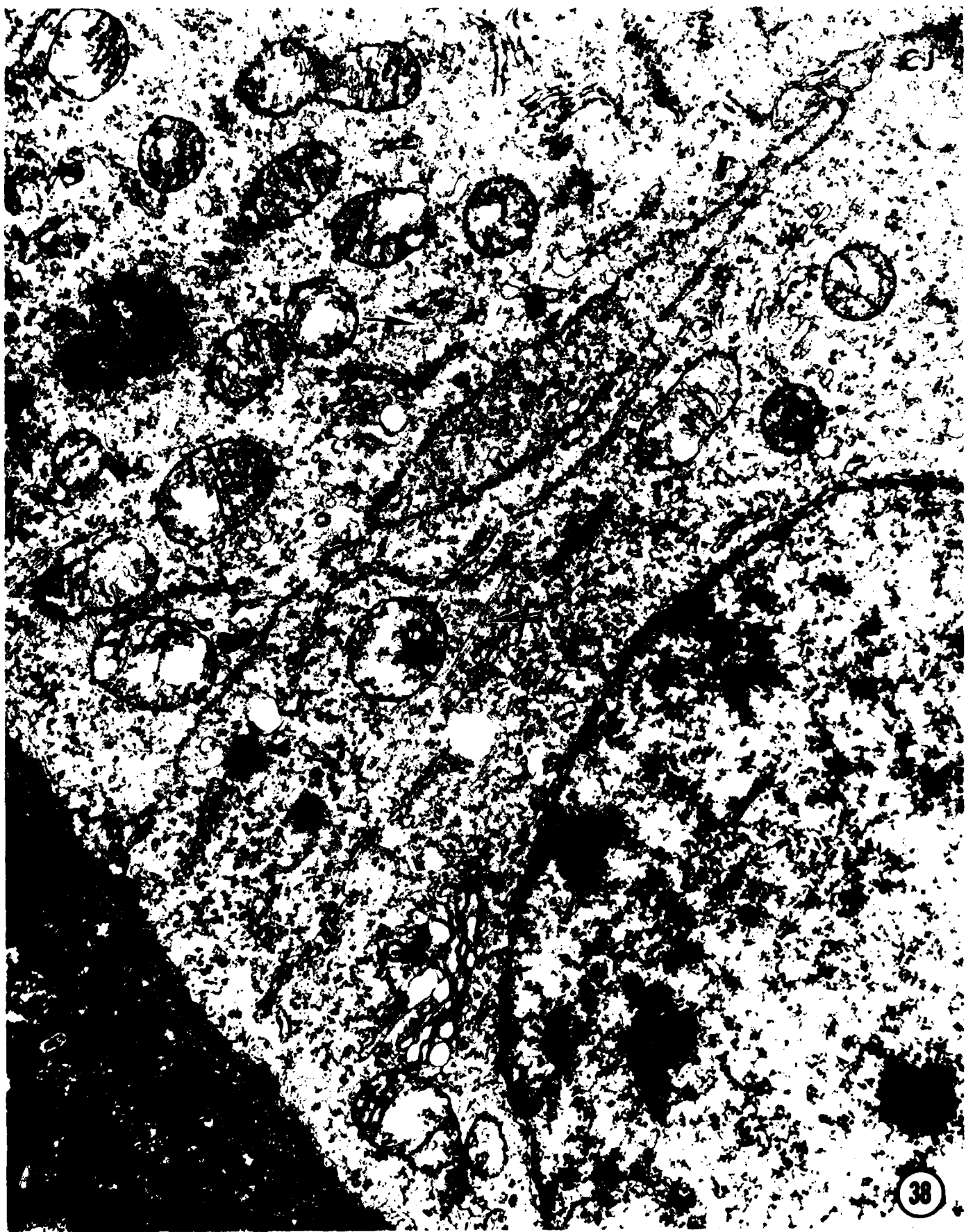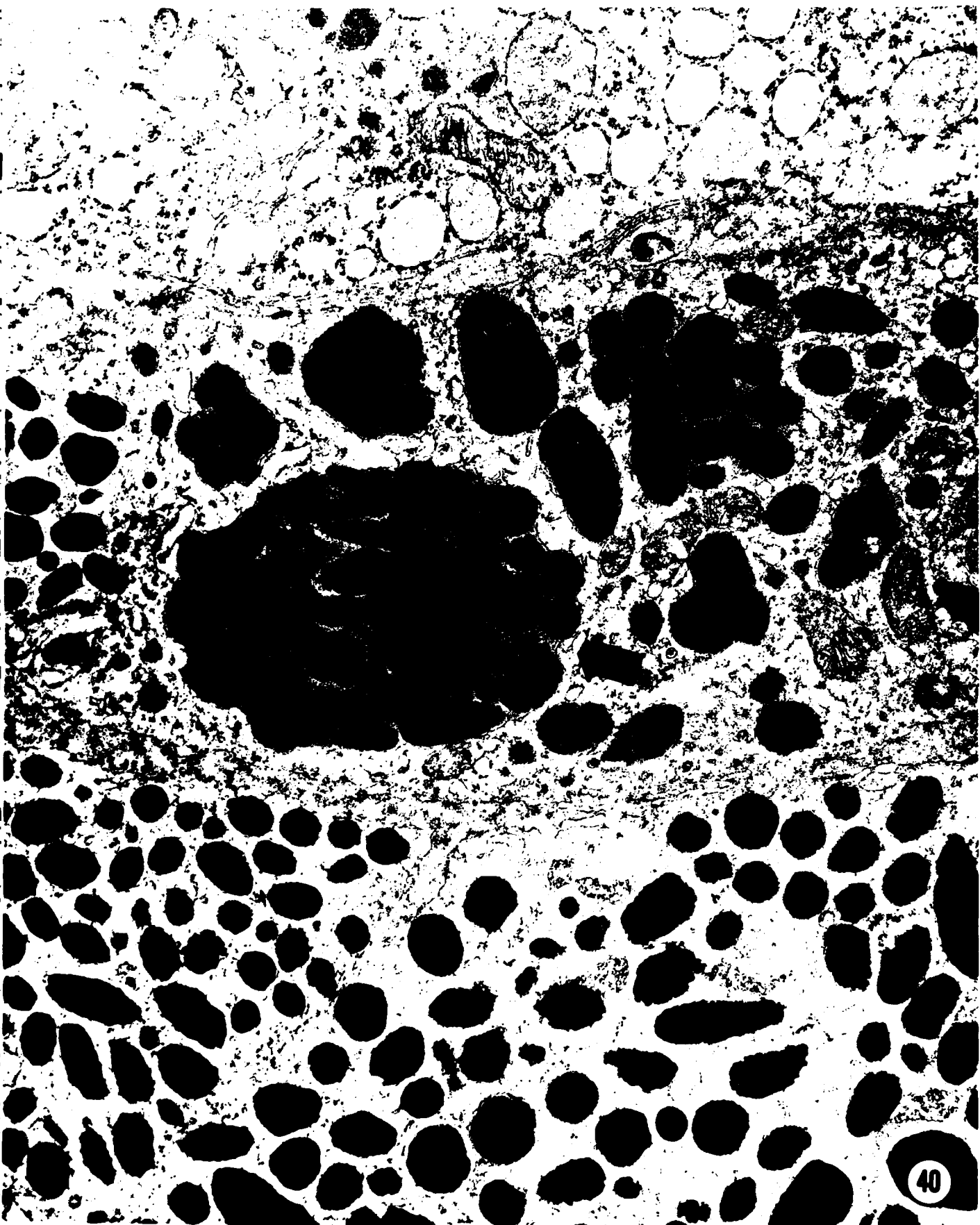
APPENDIX A

Ham, William T., Jr.; Ruffolo, John J.; Mueller, H.A.;
    Clark, A.M.; Moon, M.E. Histological Analysis of
    Photochemical Lesions Produced in Rhesus Retina by
    Short Wavelength Light. Invest. Ophthalmol. and
    Vis. Sci. 17:1029-1035; 1978.

APPENDIX B

PHOTOPATHOLOGY OF RETINAL LESIONS IN RHE-
SUS MONKEYS INDUCED BY EXTENDED EXPO-
SURE TO BLUE LIGHT AT LEVELS OF IRRADI-
ANCE BELOW THRESHOLD FOR THERMAL
EFFECTS—J. J. Ruffolo, Jr., H. A. Mueller, and W. T.
Ham, Jr., *Medical College of Virginia, Richmond, Va.*

Retinal lesions in rhesus monkeys were produced with
a 2,500 W xenon lamp optical system using narrow-band-
pass filters at 441.6 and 435.8 nm and an image size on
the retina 1 mm in diameter. The threshold of retinal
irradiance to give a funduscopically visible lesion 2 days
after exposure at paramacular locations after a 1,000 sec
exposure is approximately 30 mW/cm². Dosage reciprocity
holds for exposure times of 1,000 and 10,000 sec, with a
threshold of radiant exposure at approximately 30 J/cm²
on the retina. The histopathology of the paramacular
response to photic insult has been studied at postexposure
times ranging from less than 1 hr to 90 days. The photo-
pathology (and behavior of the funduscopic lesion) is
characterized by the response of the pigment epithelium
as pigment epitheliitis or pigmentary retinochoroiditis.
Stages of the development and regression of the para-
macular lesions will be described in detail to indicate
the relative responses of the RPE and neural retina to
photic insult. The macular response is not yet fully
described, but we have determined that the threshold
radiant exposure for a 2-day lesion is 35-45 J/cm² for
1,000 sec exposure. A higher macular threshold is pre-
sumably due to the presence of the yellow macular pig-
ment. At 60 J/cm² the 2- and 5-day macular lesions are
very similar to 2- and 5-day paramacular lesions at 33-35
J/cm². The photochemical events leading to the inflamma-
tory response are not understood.

Invest. Ophthalmol. Vis. Sci. (Suppl. 1978)
(Presented at ARVO meeting at Sarasota, Florida,
May 1978)

APPENDIX C

Moon, M.E.; Clarke, A.M.; Ruffolo, J.J.; Mueller, H.A.;
    Ham, W.T., Jr. Visual Performance in the Rhesus
    Monkey After Exposure to Blue Light. Vision
    Research. 18:1573-1577; 1978.

APPENDIX D

Ham, William T., Jr.; Mueller, Harold A.; Ruffolo,
    John J.; Clarke, A.M. Sensitivity of the Retina to
    Radiation Damage as a Function of Wavelength.
    J. Photochem. and Photobiol. 29:735-743; 1979.

END

FILMED

DTIC